GRAVITATIONAL COLLAPSE AND WEAK INTERACTIONS

W. David Arnett

Institute for Space Studies
Goddard Space Flight Center, NASA
New York, New York

I

Abstract

The behavior of a massive star during its final catastrophic stages of evolution has been investigated theoretically, with particular emphasis upon the effect of electron-type neutrino interactions. The methods of numerical hydrodynamics, with coupled energy transfer in the diffusion approximation, were used. Gravitational collapse initiated by electron-capture and by thermal disintegration of nuclei in the stellar center is examined, and the subsequent behavior does not depend sensitively upon which process causes the collapse.

As the density and temperature of the collapsing stellar core increase, the material becomes opaque to electron-type neutrinos and energy is transferred by these neutrinos to regions of the star less tightly bound by gravity. Ejection of the outer layers of the star can result. This phenomena has been identified with supernovae.

Uncertainty concerning the equation of state of a hot, dense nucleon gas causes uncertainty in the temperature of the collapsing matter. This affects the rate of energy transfer by electron-type neutrinos and the rate of energy lost to the star by muon-type neutrinos.

II

The effects of general relativity do not appear to become important in the core until after the ejection of the outer layers.

Introduction

The behavior of a massive star during its final catastrophic evolution has been investigated theoretically, with particular emphasis upon the effect of electron-type neutrino interactions. Colgate and White (1964) have suggested that the gravitational collapse of such a star may be partially reversed by a combination of shock phenomena and energy transfer by neutrino diffusion from a hot, ultra-dense core. The resulting ejection of hot matter has been identified with supernovae. The Von Neuman-Richtmeyer pseudo-viscosity method of numerical hydrodynamics, coupled with energy transfer in the diffusion approximation, has been used to investigate this hypothesis.

In section I the physical processes involved in the collapse, and the gravitational stability of a massive star are discussed. In particular, the problems of constructing an equation of state and determining the energy transfer by neutrinos under the extreme densities and temperatures to be encountered are considered. Following this, section II develops the initial models and presents their subsequent histories. Three methods of treating neutrino energy transfer - (1) no energy loss, (2) energy loss by electron pair-annihilation and plasmon decay neutrinos, and (3) thermal diffusion of neutrinos - are presented, and the results contrasted.

The effect of initial structure upon subsequent history is examined. The behavior of these models is compared with the work of Colgate and White (1964).

Section III contains an examination of the implications of the calculations reported in II, and section IV is a critique of the methods employed in the calculations. Details of the numerical techniques of hydrodynamics and energy transfer are presented in an appendix.

1. Physical Processes

In order to maintain its luminosity a star may derive energy from two sources: thermonuclear reactions and gravitational contraction. In the latter case the star converts its gravitational potential energy into kinetic energy of gas particles on such a slow time scale that hydrostatic equilibrium is approximately satisfied. No nuclear fuel can last indefinitely, so one expects that eventually the star will contract to higher densities. At these higher densities the Pauli exclusion principle can become operative and contribute to the pressure. However Chandrasekhar (1939) has shown that for electrons the maximum mass of a body supporting itself by degeneracy pressure is less than 1.5 solar masses.* If the mass of a star is less than the Chandrasekhar limit, it may radiate away its remaining thermal energy and settle down as a white dwarf. For more massive stars the situation is not so simple.

A massive star spends most of its life burning hydrogen and helium.** Helium-burning produces oxygen and perhaps some carbon (Deinzer (1964)). Fowler and Hoyle (1964) have discussed in detail the nuclear reactions occurring in subsequent evolution.

---

* For pure hydrogen the limit is higher, (see Chandrasekhar (1939), p. 423) but a pure hydrogen star is unrealistic when the Fermi energy of electrons is higher than the beta-decay energy of the neutron.

** See Hayashi (1962), Hofmeister (1964), and Stothers (1965).

After carbon-burning (temperature~8×10^8 ^oK) neutrino production by plasmon decay and electron-positron pair-annihilation robs the star of significant amounts of energy. This speeds the evolution of the star. Chiu (1964) has calculated some models of pre-supernova stars including this effect.

There are at least two mechanisms by which the star can be robbed of internal energy faster than it can replace the lost energy by quasi-static gravitational contraction. They are thermal disintegration of nuclei and electron-capture. When these mechanisms operate, the star will collapse, falling almost freely in its own gravitational field. Which process will actually trigger the collapse depends on the details of pre-implosion evolution.

A. Thermal Disintegration of Nuclei

For temperatures greater than $T = 4 \times 10^9$ ^oK and densities the order of or greater than $\rho = 10^6$ gm/cm^3 a wide variety of nuclear reactions can occur. A calculation of these rates requires an accurate knowledge of the initial nuclear composition of the matter, a large collection of nuclear parameters,* and considerable effort. It is beyond the scope of this work to justify a pre-supernova model involving such a calculation.

* See Truran, Hansen, Cameron, and Gilbert (1965), for instance.

If the reactions are fast enough, the problem may be treated by the methods of statistical equilibrium. Insofar as the equation of state is concerned, the only changes of interest are those which are strongly endoergic or exoergic. The photodisintegration of ^{56}Fe matter in the implosion has been discussed by Fowler and Hoyle (1964). They find that for temperatures $T \geq 7.10^9\ ^oK$ that the photodisintegration time is $t \sim 10^{-6}$ second --- which is no larger than the most restrictive hydrodynamic time scale. Hoyle and Fowler note that the equilibrium composition for ^{56}Fe matter changes to essentially pure ^4He in a region of width

$$\Delta T \sim 1 \times 10^9\ ^oK$$

about the density-temperature curve corresponding to an equilibrium concentration of half ^{56}Fe, and half ^4He and neutrons, i.e., the curve

$$\log \rho = 11.62 + 1.5 \log T_9 - \frac{39.17}{T_9}$$

where T_9 means temperature in units of one billion degrees, logarithms are to the base 10 and density ρ is in gm/cm^3. This may be approximated by the expression

$$T_9/6.0 = (\rho/1.82 \times 10^6\ gm/cm^3)^{0.081}.$$

For somewhat higher temperatures photodisintegration of alpha particles is expected.

$$^4He \rightarrow 2p + 2n$$

In this case the transition region is approximated by

$$T/(12\times10^9\ {}^{o}K) = (\rho/(10^8\ gm/cm^3))^{0.13}$$

Now the energy required to produce the reaction

$$^{56}Fe \rightarrow 13\ ^{4}He + 4n$$

is

$$Q(Fe,\alpha) = -2.1\times 10^{18}\ erg/gm$$

and for

$$^{4}He \rightarrow 2p + 2n$$

is

$$Q(\alpha,np) = -6.8\times 10^{18}\ erg/gm$$

These values will be roughly correct even if the composition is not ^{56}Fe, but some other stable nuclide. Subsequent results will not depend sensitively upon this choice.

B. Electron-capture

Consider a nucleus (Z,A) which is stable against beta-decay on earth. It may be a product of some reaction represented by

(1) $$(Z-1,A) \rightarrow (Z,A) + e^- + \bar{\nu}.$$

Under stellar conditions of extreme density an endothermic reaction of the form

(2) $$(Z,A) + e^- \rightarrow (Z-1,A) + \nu$$

can occur in which the terrestrially stable nucleus (Z,A) is induced to capture a continuum electron from the surrounding plasma.

Bahcall (1964c) has investigated this process and finds that for allowed decays, the half-life for the process (2) in a stellar interior is related to the half-life for the decay (1) on earth by

$$(\tau_{1/2})_{star} = (f\tau_{1/2})_{lab} K^{-1}$$

where f is the usual function used in the comparative half life, i.e.,

$$f(\pm Z,W) = \int_0^{p_{max}} dp\ p^2\ F(\pm Z,W)$$

and p is electron momentum, W is relativistic electron energy, q is the neutrino momentum and $F(\pm Z,W)$ is the Fermi function. Now

$$K = \int_{p_{threshold}}^{\infty} dp\ p^2\ q^2\ F(Z,W)/(1+e^{(W-\mu)/kT})$$

(where μ is the relativistic chemical potential) is the appropriate generalization of $f(+Z,W)$ for reaction (2). The range of integration now extends from the electron momentum corresponding to the threshold energy of (2) to all higher energies. The correct weighing factor for a Fermi-Dirac distribution of electrons,

$$(1 + \exp[\ (W-\mu)/kT]\ )^{-1},$$

is included. The integral K will be large compared to $f(+Z,W)$ when the electron distribution is such that energy levels with

$$W \geq W_{threshold}$$

for the capture reaction, are well populated. This can occur in

the nondegenerate case when

(3) $$kT \gtrsim W_{\text{threshold}}$$

and in the degenerate case when

(4) $$W_{\text{Fermi}} \gtrsim W_{\text{threshold}}$$

Taking $W_{\text{threshold}}$ to be the order of nucleon binding energy in the nuclear potential should give an estimate of the thermodynamic conditions under which induced electron capture will begin to occur. If we take the threshold for the electron capture to be

$$W_{\text{threshold}} \sim 8 \text{ MeV},$$

then for a nondegenerate gas, the condition (3) implies that the temperature is

$$T \gtrsim 10^{11} \, {}^{o}K,$$

but thermal disintegration discussed in the previous section will have already disrupted the nuclei at much lower temperatures. Using (4) gives a condition* on the density ρ

$$\frac{\rho}{\mu_e} \gtrsim 10^9 \text{ gm/cm}^3.$$

* The quantity μ has its usual astrophysical definition of average atomic weight per free particle ($\mu_e = A/(Z + 1)$ for a completely ionized gas).

Beyond this density nuclei will capture high energy electrons from the top of the Fermi sea. The alpha particle, ^4He, will be extremely resistent to electron capture because there is no stable nucleus with Z = 1, A = 4, whereas the α particle is tightly bound. The threshold for electron capture on ^4He will be of the order of the energy needed to disintegrate the nucleons, i.e., about 30 MeV for complete disruption, but the reaction of most importance is probably

$$^4He + e^- \rightarrow {}^3H + n + \nu_e$$

which requires about 21 MeV. A value for the electron Fermi energy of 30 MeV corresponds to a density of the order of

$$\frac{\rho}{\mu_e} \sim 2 \times 10^{11} \text{ gm/cm}^3$$

As the density rises, so that the Fermi energy becomes greater than the threshold energy, the continuum electron capture rates increase until an assembly composed predominantly of neutrons is formed.

C. Stability Against Continued Implosion

Once the implosion begins it cannot be stopped until the pressure is again large enough to provide mechanical support for the configuration. Chandrasekhar (1939) has shown that the boundary for mechanical stability of a self-gravitating mass is

the $\gamma = 4/3$ adiabat. That is, if upon compression the change in pressure and density of the material can be represented by

$$\gamma = d(\log P)/d(\log \rho)$$

then for $\gamma > 4/3$ the material is stable, but for $\gamma < 4/3$ the material is unstable toward continued contraction.* As particles become relativistic the relation between energy and momentum changes from

$$\epsilon = \frac{p^2}{2m}$$

to

$$\epsilon = pc$$

in the extreme relativistic case. The corresponding relations for a gas of such particles are

nonrel.	rel.
$E = \frac{3}{2} PV$	$E = 3 PV$
$\gamma = 5/3$	$\gamma = 4/3$

*Actually the criteria are somewhat more complicated, dealing with pressure averages of γ. F. Dyson, "Hydrostatic Instability of a Star," unpublished.

where E is the energy density per unit mass, P the pressure and $V = 1/\rho$ the specific volume. Thus, as the temperature (or the Fermi energy) increases we expect the effective adiabatic exponent of the gas, γ , to approach four-thirds. At what temperature this occurs depends upon the rest mass of the gas particles (photons, having zero rest mass are always relativistic, electrons become relativistic for $T \sim 6 \times 10^9$ ^oK, while nucleons require $T \sim 1.2 \times 10^{13}$ ^oK). Large amounts of energy are removed from the star by neutrino emission. Both the processes of electron-capture and thermal disintegration of nuclei require large amounts of energy to proceed; in both cases this energy is at least of the order of nuclear binding energy. In view of these large energy requirements, the material is expected to become degenerate even if it was not originally so.

The problem of stability against continued collapse is then reduced to whether a cold, dense neutron gas can give a pressure contribution which increases with density faster than $\gamma = 4/3$. From investigation of the properties of nuclear matter such a contribution is found.

D. The Equation of State

At densities of the order of or less than nuclear densities ($\rho \lesssim 3 \times 10^{14}$ gm/cm^3) the attractive nuclear potential lowers

the pressure below that expected for a degenerate, noninteracting gas of fermions. The nuclear potential becomes strongly repulsive at higher densities, and raises the pressure above that expected for a noninteracting gas, but the exact details of nuclear potentials in this range (greater than nuclear density) is not well known. From the several forms of the nuclear potential discussed by Tsuruta (1964), it appears that there will be a pressure term of the form

$$P \sim \rho^{\gamma}$$

where

$$\gamma \gtrsim 2$$

These results for the equation of state are based on the assumption that the nucleons may represent a noninteracting, degenerate gas of Fermi particles in a common potential well.

Bahcall and Wolf (1965) have attempted to determine the effect of nucleon-nucleon interactions more accurately by using the "independent-pair" model of Gomes, Walecka and Weisskopf (1958). This technique is valid only if the nucleons are highly degenerate. Unfortunately it is necessary to know the equation of state for nondegenerate and semi-degenerate nucleon matter. In view of the uncertainties involved in any nuclear equation of state and the numerical limitations of this investigation, and extremely simple form for nuclear pressure at high density and temperature was chosen: The nucleons were assumed to be a gas of noninteracting,

free Fermi particles. This reproduces the correct general character in the limits of complete degeneracy and of high temperature, low density. In order to avoid excessive use of computer time, the equation of state was constructed from a composite of analytic terms.

In addition to the nucleon pressure terms discussed above, black-body radiation pressure and electron pressure (including relativistic degeneracy) were taken into account. Thus the approximate expression for the pressure is

$$P = R\left(\frac{\rho}{\mu_n}\right) T + K_n\left(\frac{\rho}{\mu_n}\right)^{5/3}$$

$$+R\left(\frac{\rho}{\mu_e}\right) T + K_e\left(\frac{\rho}{\mu_e}\right)^{4/3} + \frac{aT^4}{3}$$

where R is the gas constant, the constants K_e and K_n are

$$K_e = 1.201 \times 10^{15} \text{ dynes cm}^{-2}$$

$$K_n = 5.226 \times 10^{9} \text{ dynes cm}^{-2}$$

if the density ρ has units gm cm^{-3}, T is the temperature, and the number density of the $i^{\underline{th}}$ type of particle (n = neutron, e = electron) is

$$N_i \sim \frac{\rho}{\mu_i} N_a$$

where N_a is Avagadro's number. The number density of neutrons is negligible before electron capture occurs. Electron-pair

creation does not affect the equation of state for large electron number density. The energy density corresponding to this pressure has the simple form

$$E = \sum_i \frac{P_i V}{(\gamma_i - 1)}$$

where $\gamma = 4/3$ for the relativistic particles and $\gamma = 5/3$ for nonrelativistic ones.

Electron capture reactions were accounted for as follows: Since the expression

$$\frac{\rho}{\mu_e} = \frac{1}{V \mu_e} \sim n_e$$

is proportional to the number density of electrons, smoothly changing μ_e provides a convenient way to reduce the electron pressure of the system. When the relativistic electron Fermi energy E_f,

$$\frac{E_f}{m_e c^2} \approx \left(\frac{\rho_6}{\mu_e}\right)^{1/3}$$

where ρ_6 is density in units of 10^6 gm/cm^3, reaches a given level, the number density of electrons is held constant until the degenerate nucleon pressure becomes more important. That this agrees with other estimates may be seen in Figure (1). Two parameters are involved: the Fermi energy at which captures are supposed to occur, and the factor by which the electron number density is decreased.

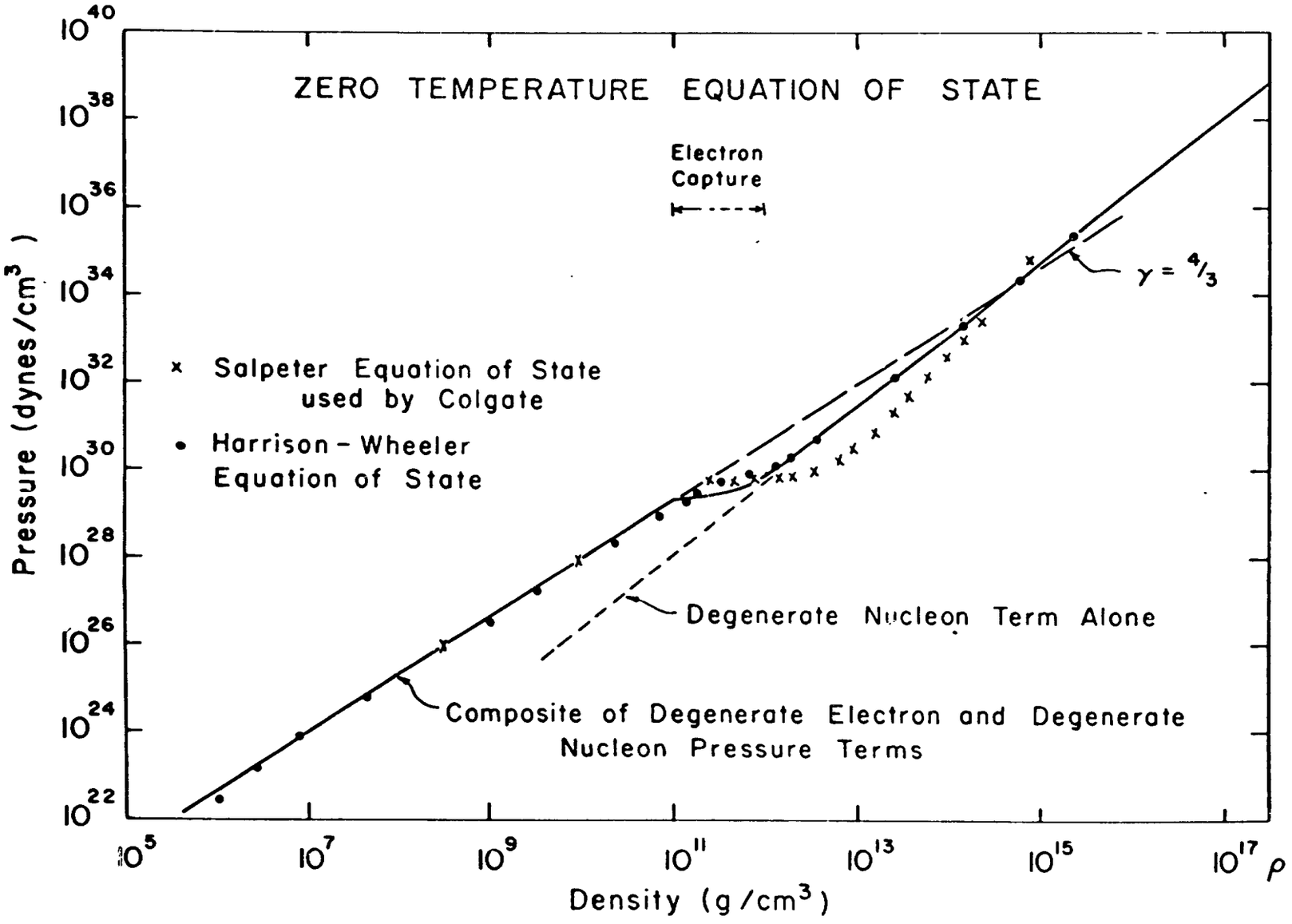
ZERO TEMPERATURE EQUATION OF STATE
Electron Capture
Salpeter Equation of State used by Colgate
Harrison - Wheeler Equation of State
$\gamma = 4/3$
Degenerate Nucleon Term Alone
Composite of Degenerate Electron and Degenerate Nucleon Pressure Terms
Pressure (dynes/cm^3)
Density (g/cm^3)
10^{40}
10^{38}
10^{36}
10^{34}
10^{32}
10^{30}
10^{28}
10^{26}
10^{24}
10^{22}
10^5
10^7
10^9
10^{11}
10^{13}
10^{15}
10^{17}
ρ

Actually the onset of electron capture reactions is a gradual process, beginning at densities as low as 10^9 gm/cm^3. Figure (1) shows that the Harrison-Wheeler* equation of state gives a slightly lower pressure than expected from a relativistic electron gas at densities from about 10^9 to 10^{11} gm/cm^3 because of electron capture. Tsuruta (1964) finds that the equilibrium abundance peak of zero temperature matter shifts from ^{56}Fe at low density ($\sim 10^7$ gm/cm^3) to very neutron-rich heavy nuclei at higher density ($\gtrsim 10^{11}$ gm/cm^3) due to electron capture. The effect of this is to initiate a contraction in a pre-supernova star at much lower densities than might be expected otherwise. The assumption of a sharp electron capture threshold is unrealistic, but is probably a minor source of error. In the calculations to be reported, electron capture was assumed to occur rapidly when the Fermi energy was slightly above the 21 MeV or so necessary to drive the reaction

$$^4\text{He} + e^- \rightarrow {}^3\text{H} + n$$

that is, for $\rho \sim 10^{11}$ gm/cm^3.

---

* Harrison, B. K., et al, 1965, chapter 10.

As Figure (1) shows, a zero-temperature body undergoing quasi-static gravitational contraction will encounter a pressure deficit at densities above $\rho \sim 10^{11}$ gm/cm^3. The equation of state does not compensate for this pressure loss relative to a $\gamma = 4/3$ adiabat until the density is about 10^{15} gm/cm^3. This is accomplished here by approximating the complicated equation of state for nuclear matter by that of a noninteracting non-relativistic Fermi gas. In the region where the pressure deficit occurs, $10^{11} < \rho < 10^{15}$ gm/cm^3, the detailed nature of the equation of state is relatively unimportant because the supernova core is falling in freely to higher densities and is not affected by the nucleon pressure contribution. In this region Tsuruta's equation of state gives pressures between those of the Harrison-Wheeler and the Salpeter equation of state, except when a nuclear hard-core term begins to dominate the equation of state. It should be emphasized that the zero-temperature equation of state is only a convenient limiting case, and that finite temperature effects are important in supernovae collapse.

E. Neutrinos and Energy Transfer

The effectiveness of a given mechanism for energy transfer depends on the rate at which energy can be put into the given mode, and on the speed with which the given mode moves this energy. Energy transfer in stars is generally accomplished by photon

diffusion, or in some cases by convective mass motion or conduction by degenerate electrons (see Schwarzschild, 1958). Using the Thomson cross-section for the electron, the photon mean free path is roughly

$$\lambda \text{ photon} \sim \frac{1}{N_e \sigma_{th}} \sim \frac{1}{\rho} \text{ cm.}$$

where N_e is the electron number density per unit volume, σ_{th} is the Thomson cross-section, and ρ is the density in gm/cm^3. For the core of a star with a central density of, say, 10^6 gm/cm^3, the time for a photon to diffuse through even ten kilometers of matter is

$$\tau \text{ ph.dif.} \sim \frac{\Delta R^2}{\lambda c} \sim 10 \text{ years.}$$

The universal theory of weak interactions* of Feynman and Gell-Mann (1958) predicts a large number of processes that result in the formation of neutrino-antineutrino pairs. The emission of a neutrino pair is much less probable than the emission of a photon so that the process is not generally observable in the laboratory. Once formed, however, the neutrino pair is virtually certain to escape from a normal star ($\rho_{\text{central}} \ll 10^{11}$ gm/cm^3). For temperatures less than several billion degrees, the cross-section for neutrinos and antineutrinos is roughly

$$\sigma \sim 10^{-44} \text{ cm}^2.$$

so that the mean free path is

$$\text{neutrino} \sim \frac{10^{20}}{\rho} \text{ cm.}$$

*Or any theory which predicts coupling of terms of the form $(\bar{\nu}e)(\bar{e}\nu)$.

which is roughly 100 light years for the density of the sun. Thus, excluding extreme conditions, the production of neutrinos acts as an instantaneous local energy sink for the star.

1. Energy Loss by Neutrino Escape.

Chiu (1961) has calculated the energy loss rate due to the process

$$e^+ + e^- \rightarrow \bar{\nu} + \nu$$

for stellar material in the temperature range (0.5 to 10) x 10^9 ^oK and densities (0 to 10^9 gm/cm^3). In much of this range the electrons are partially degenerate and numerical evaluation of integrals was necessary. Analytic forms for limiting cases have been presented by Chiu and Stabler* (1961).

For

$$mc^2 \ll kT$$

and

$$E_{Fermi} \lesssim kT$$

the energy loss rate is

$$Q = 4.3 \times 10^{15} \frac{(T_9)}{\rho} \text{ ergs/gm/sec}$$

where ρ is in gm/cm^3 and T_9 is the temperature in units of 10^9 ^oK.

* See Ritus (1962) for a numerical correction of the photoneutrino rates in this paper.

This approximation is inaccurate when temperatures are about 3×10^9 ^oK or below, but the energy loss rates are then too small to affect the hydrodynamic calculation. The approximation is also invalid when degeneracy is pronounced, but then the plasmon-neutrino loss rate is larger, so that the numerical error is negligible.

The production of neutrino pairs by coherent electron excitations (transverse plasmons) in a hot, partially degenerate relativistic plasma has been calculated* by Adams, Ruderman and Woo (1963), and extended by Inman and Ruderman (1964). Neutrino-pair emission by collective electron modes, especially transverse plasma excitations, is found to be the main mechanism for neutrino radiation by a dense plasma when electron-positron production is small either because the temperature is too low or degeneracy suppresses it. Chiu (1964) gives an analytical approximation for the plasma neutrino process:

$$Q = -1.1 \quad (T_9)^3 \quad \rho \text{ erg/gm/sec.}$$

where the usual notation is employed. This is valid for

$$x \leq 1$$

where x is given by

$$x = 0.237(1 + 0.6413(\rho_6)^{2/3})^{-1/4} \quad (\rho_6)^{1/2}$$

if

$$\rho_6 >> 1$$

* Zaidi has recently indicated that this rate is too large by a factor of 4 (to be published).

The density ρ_6 has units of 10^6 gm/cm^3. Actually numerical evaluation of the pair annihilation, plasma and photoneutrino rates by Hansen (1964) indicates that this approximation is reasonably good (factor of 2) for densities as high as 10^{11} gm/cm^3 or so if the temperature is $T \leq 10^{10}$ ^oK. Again, errors in small energy-loss rates are negligible from a hydrodynamic point of view. For temperatures much higher than this the pair annihilation rate is dominant, so that the approximation is reasonable in the region in which it is the primary energy loss mechanism.

The plasmon-decay and the pair-annihilation energy loss rates are of interest for two reasons. First, they may be important in cooling shock-ejected matter whose density is less than $\rho \sim 10^{11}$ gm/cm^3. Also, for higher densities other neutrino processes will probably dominate, but these processes nevertheless provide a convenient estimate of the minimum possible energy loss rate which is not plagued by the uncertainties* in the effect of strong interactions.

2. Neutrino Opacity.

The interactions of neutrinos and antineutrinos in dense matter have been discussed by Bahcall (1964a), Bahcall and Frautschi (1964b) and Euwema (1964). Euwema calculates the inhibiting factor for effects of the exclusion principle on neutrino absorption.

* See Bahcall and Wolf (1965) for example.

Negligible temperature and completely noninteracting particles which filled all states below the Fermi level and none above, were assumed. Bahcall and Frautschi have considered neutrino-lepton scattering and neutrino-nucleon interactions generally. In particular, Bahcall (1964a) has suggested that neutrino-electron scattering

$$\nu_\beta + e^- \rightarrow \nu_\beta' + e^{-\prime}$$

$$\bar{\nu}_\beta + e^- \rightarrow \bar{\nu}_\beta' + e^{-\prime}$$

is the most important neutrino process for energy deposition in the supernova model of Colgate and White (1964).

a) Nondegenerate gas.

For a nondegenerate gas of electrons, the total cross-section averaged over the initial electron distribution is

$$(\sigma)_{\omega,p} = \left[4\pi^3 n_e \left(\frac{\hbar}{mc}\right)^3 \right]^{-1} \int d^3p \left[1 + e^{(W-\mu)/kT}\right]^{-1} \sigma(p_\alpha, \omega_\alpha)$$

where $\sigma(p_\alpha, \omega_\alpha)$ for neutrino-electron scattering is

$$\sigma(p_\alpha, \omega_\alpha) = \sigma_o (p_\alpha \cdot \omega_\alpha)^2 / (1 + 2p_\alpha \cdot \omega_\alpha)$$

and for antineutrino electron scattering is

$$\sigma(p_\alpha, \omega_\alpha) = \sigma_o \left(\frac{p_\alpha \cdot \omega_\alpha}{6}\right) \left[1 - (1 + 2p_\alpha \cdot \omega_\alpha)^{-3}\right]$$

where n_e is the electron number density per unit volume, p is the electron momentum, W the total electron energy, p_α the dimensionless

four-momentum of the electron, ω_α the corresponding four-momentum for the neutrino, and μ the chemical potential of the electrons. The constant σ_o is

$$\sigma_o = \frac{4}{\pi} \left(\frac{\hbar}{m_e c}\right)^{-4} \left(\frac{G}{m_e c^2}\right)^2$$

$$\approx 1.7 \times 10^{-44} \text{ cm}^2.$$

In the case $kT >> m_e c^2$, the thermal motion of the electrons produces a large center-of-mass energy and hence causes the cross-section to exceed greatly the cross-sections for electrons at rest. In this limit Bahcall finds, for neutrino energies $E_\nu >> m_e c^2$, that

$$(\sigma)_{\omega,T} \simeq 3.2 \, (kT/m_e c^2) \, \frac{\sigma_o \omega}{2}$$

for the neutrino, and for the antineutrino

$$\frac{\sigma_o \omega}{2} \rightarrow \frac{\sigma_o \omega}{5}.$$

Bahcall gives the following form for the neutrino energy loss per scatter

$$\frac{(\omega - \omega')_{av.}}{\omega} \approx \frac{1}{2} \left[1 - \frac{4kT}{\omega m_e c^2}\right]$$

where ω is the dimensionless neutrino energy and the prime refers to the quantity after collision. This approximation requires

$$\omega >> 1 \text{ and } kT >> m_e c^2$$

For sufficiently high electron temperatures, the neutrinos gain more energy per collision on the average than they lose.

b) Degenerate Gas.

In a degenerate electron gas both the initial electron distribution and the prior occupation of final electron states must be considered. Bahcall (1964a) gives the general expression for neutrino-electron scattering as

$$\sigma_\omega = \frac{\sigma_o}{4\pi}\left[4\pi^3 n_e \left(\frac{\hbar}{m_e c^2}\right)^3\right]^{-2} \iiint \left[d^3p \frac{d^3\rho\, d^3\omega'}{\epsilon'\omega'}\right.$$

$$\left. S(\epsilon)[1 - S(\epsilon')](P'_\alpha \quad \omega'_\alpha) \quad \delta^{(4)}(P_\alpha+\omega_\alpha-P'_\alpha-\omega'_\alpha)\right]$$

where ϵ is the dimensionless electron total energy and the other notation is as before, except for

$$S(x) \equiv [1 + \exp([x-\mu]/kT)]^{-1}$$

where μ is the electron chemical potential. For a completely degenerate gas,

$$S(\epsilon) = 1 \text{ for } \epsilon < E_f$$

$$= 0 \text{ for } \epsilon > E_f$$

where E_f is the total Fermi energy. Bahcall estimates

$$\sigma(\omega', E_f) \approx \begin{cases} \sigma_o \omega^2 & \omega << E_f \\ \sigma_o E_f \omega & \omega >> E_f \end{cases}$$

and for antineutrino scattering the results are multiplied by 1/3.

The results of Bahcall and Frautschi (1964b) indicate that for

$$N_e > 10^{-2} N_n$$

that is, for the electron number density more than 1% of the nucleon number density, neutrino-nucleon scattering is less than neutrino-electron scattering, and will be neglected.

The situation is not clear concerning neutrino absorption by nucleons. In the "low" density domain ($\rho < 3 \times 10^{14}$ gm/cm^3) nucleons not bound in nuclei will display the cross-section

$$\sigma(\omega) \approx \sigma_o \omega^2$$

for neutrinos with energy much larger than $m_e c^2 \sim 0.5$ MeV. For lower energies the behavior is more complicated, with the reaction

$$\bar{\nu} + p \rightarrow n + e^+$$

having a threshold while the reaction

$$\nu + n \rightarrow p + e^-$$

does not. For densities greater than or the order of nuclear density ($\rho \gtrsim 3 \times 10^{14}$ gm/cm^3) the previously mentioned uncertainty with the equation of state may affect the neutrino absorption cross-section by changing the threshold energy or by reducing the phase space available to nucleons in the exit channel. In any case, the extinction cross-section for neutrinos is at least as large as that predicted by neutrino-electron scattering alone, and may be larger. If the number density of electrons becomes considerably less than that of nucleons, then the neutrino opacity of the material cannot be represented, even approximately, without knowing the neutrino-nucleon interaction cross-sections. Thus the equation of

state problem is again encountered. The opacities used in the calculations presented here are due to neutrino-electron scattering.

3. Energy Transfer by Neutrinos.

In this investigation neutrinos were assumed to transfer energy by thermal diffusion. Although tested numerical techniques for time-dependent transfer problems are available (Richtmyer, 1957) it appears that any reasonably accurate transport treatment requires too much machine time for an exploratory calculation. In addition, other approximations, such as neglect of general relativity, make a detailed study of the coupled problem inappropriate at this time. Consequently energy transfer by neutrinos was treated in the thermal diffusion approximation* with the hope that the accuracy would be on the level attained by other aspects of the calculation.

The thermal diffusion approximation assumes that the diffusing energy carriers (usually photons, but in this case electron-type neutrinos and their anti-particles) are in thermal equilibrium with the medium through which they move. The anisotropy which drives the energy transfer is assumed to be a perturbation on a generally isotropic distribution of carriers. The assumption of thermal equilibrium avoids detailed consideration of the processes of neutrino formation, a neglect which greatly simplifies the problem.

---

* The approach in this section follows that of Frank-Kamenetskii (1962) for photons.

The first law of thermodynamics can now be expressed as

$$dE = (\dot{s} - \frac{\partial L}{\partial M}) \, dt - P dV$$

where E is energy density, $\dot{s}$ the rate at which thermal energy is added to the medium, P is the pressure, and V is the specific volume. Assuming spherical geometry, the mass M satisfies the equation

$$dM = 4 \pi \rho r^2 \, dr$$

where $\rho = 1/V$ is the density and r is the radius of the spherical element under consideration. The luminosity L is given by the usual expression

$$L = (4\pi r^2)^2 \frac{ac}{3\bar{K}} \frac{d(T^4)}{dM}$$

where a is the radiation constant, c the velocity of light, T the temperature and $\bar{K}$ the Rosseland mean opacity

$$\bar{K} = \frac{1}{\rho \bar{\ell}}$$

where $\bar{\ell}$ is the corresponding mean free path. Notice that for simplicity we have assumed that the neutrino and anti-neutrinos may be described by a single "black-body" Fermi gas, that is, the chemical potentials of the neutrinos and antineutrinos are zero. Using Bahcall's (1964) limiting forms for the electron-neutrino (antineutrino) cross-sections, the Rosseland mean opacities can be evaluated analytically*

---

* L.D. Landau and E.M. Lifshitz (1958) Statistical Physics.

for a "black-body" Fermi distribution. However it is sufficiently accurate to replace the neutrino energy by an average value

$$< \varepsilon_\nu > \sim 3kT$$

so that

$$\rho\bar{K} = N_e \sigma_o (3kT)^2$$

where the quantities have been defined previously.

It is interesting to note that the integrated neutrino-electron scattering cross-section for a degenerate electron gas is nonzero even if the neutrino energy ω is less than the electron Fermi energy ε_f,

$$< \sigma > \simeq \sigma_o \omega^2 \text{ for } \omega << \varepsilon_f$$

This means that there is no completely transparent window even for low energy neutrinos ($m_e c^2 << \omega << \varepsilon_f$). Very low energy neutrinos ($\omega \leq m_e c^2$) are expected to transfer little energy on short time scales.

The approximation of thermally diffusing neutrinos will be valid only if the neutrino mean free path is shorter than the distance in which the macroscopic variables change. That this condition may be satisfied can be seen as follows. For a density greater than

$$\rho \sim 10^{11} \text{ gm/cm}^3$$

the electron Fermi energy never falls below about 30 MeV, so that the electron number density is at least $N_e \sim 10^{35}$ cm^{-3}. Detailed numerical calculations show that the macroscopic variables change little over distances of the order of

$$\Delta X < 2 \times 10^6 \text{ cm.}$$

If the mean free path for a neutrino must satisfy the relation

$$\bar{l} \gtrsim \Delta X$$

then the average neutrino energy must be

$$\bar{\epsilon} \gtrsim (\Delta X \quad N_e \quad \sigma_o)^{-\frac{1}{2}} \sim 8 \text{ MeV}$$

If a thermal distribution is assumed, $\bar{\epsilon} \sim 3kT$, so that the temperature must be greater than

$$T \sim 36 \times 10^9 \text{ }^{o}K.$$

Temperatures far in excess of this are encountered. Eventually this condition breaks down at lower densities, and a "luminous surface" for neutrinos is formed, beyond which the neutrinos almost certainly escape the star without interaction. In this region the energy deposited by the incident neutrino flux and that lost by neutrinos escaping were taken into account in determining the boundary condition. Because of the rapid transition from neutrino-opaque to neutrino-transparent condition, the calculation appears to be insensitive to exact form used.

III. Hydrodynamic Calculations of Stellar Collapse.

A. Initial Models.

Models for stars just prior to supernova implosion have been suggested by Fowler and Hoyle, (1964), and by Chiu (1964). It appears that the essential differences are: (1) Chiu's model is much more centrally condensed, with a higher central density, and (2) because the central temperatures are roughly the same, the center of Chiu's model lies on a lower adiabat. The model suggested by Chiu has electron degeneracy in the core while that of Fowler and Hoyle is nondegenerate, at least until endoergic nuclear reactions become significant. Figures (2) and (3) illustrate the two approximate models chosen to reproduce these characteristics. An n = 3 polytrope, that is, a gravitating gas sphere in hydrostatic equilibrium for which the pressure and density are related by

$$\rho \sim p^{4/3}$$

was chosen to represent the Fowler-Hoyle model. The mass was ten times that of the sun and the initial radius was $R = 10^{10}$cm.

The Chiu model was approximated by an isothermal core of 1.435 $M_\odot$ and a $\gamma = 5/3$ envelope giving a total mass of 1.952 $M_\odot$. This model might correspond to the centrally-condensed core of a more massive star with giant structure,

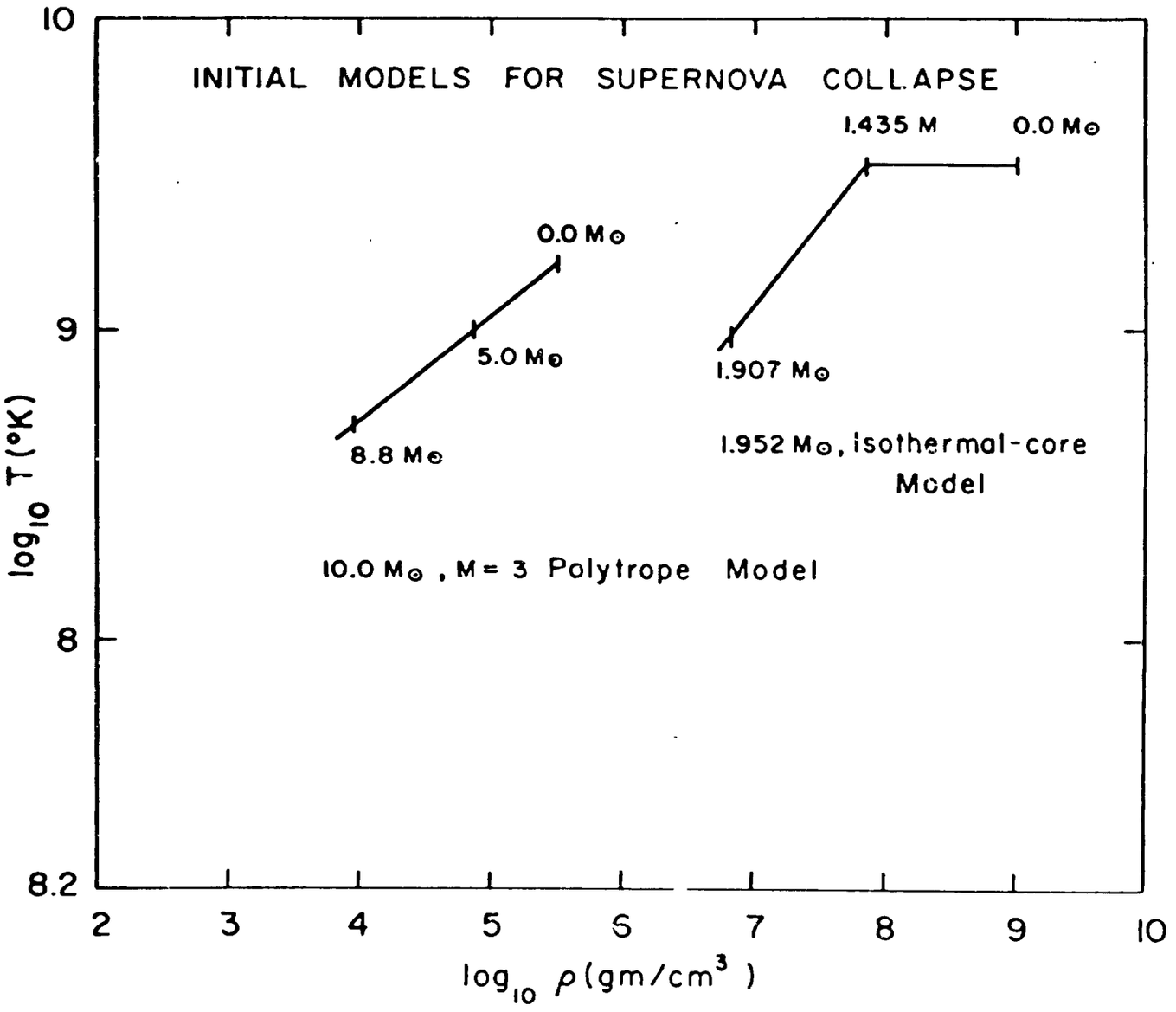
INITIAL MODELS FOR SUPERNOVA COLLAPSE
1.435 M
0.0 M⊙
0.0 M⊙
5.0 M⊙
8.8 M⊙
1.907 M⊙
1.952 M⊙, isothermal-core Model
10.0 M⊙ , M = 3 Polytrope Model
log10 T (°K)
log10 ρ (gm/cm3)
10
9
8
8.2
2
3
4
5
6
7
8
9
10

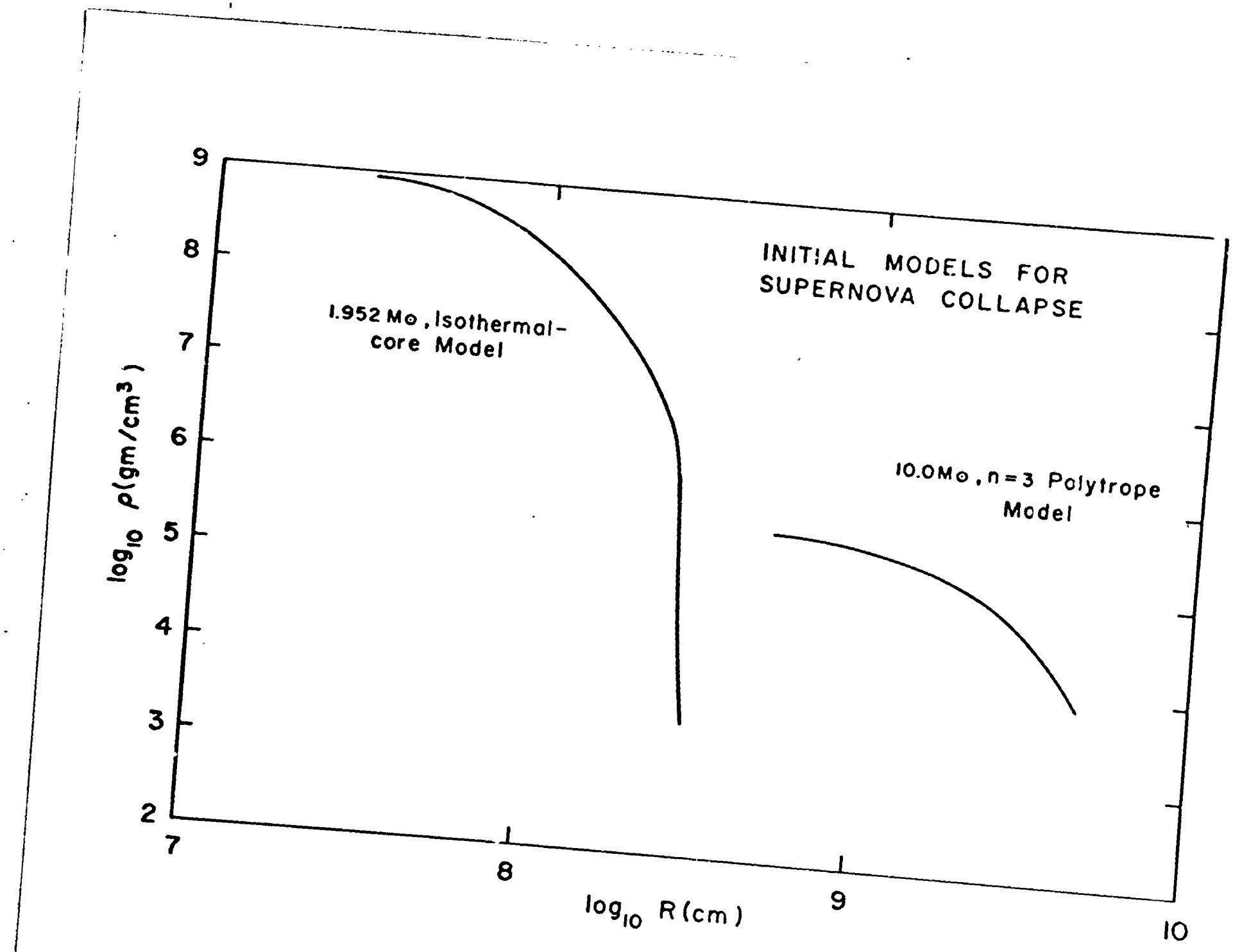
INITIAL MODELS FOR
SUPERNOVA COLLAPSE
1.952 Mo , Isothermal-
core Model
10.0Mo , n=3 Polytrope
Model
log10 ρ(gm/cm3)
9
8
7
6
5
4
3
2
7
8
9
10
log10 R(cm)

the extensive envelope being neglected. Although this is not as centrally condensed as the model with a positive temperature gradient in the core which Chiu first suggested, it does give a highly condensed structure and is in sufficient contrast with the Fowler-Hoyle model.

B. Dynamical History of $10M_{\odot}$ Pre-supernova Models of Polytropic Structure.

In order to clarify the effects of neutrino energy transfer, the following models are to be presented: (1) the "no-neutrino" model in which all neutrino energy transfer is ignored, (2) "neutrino sink" model in which all neutrinos, once formed, are assumed to escape the star without interaction, (3) "neutrino diffusion" model in which diffusive energy transfer by neutrinos at high densities and temperatures may occur. The choice of a $10M_{\odot}$ polytrope of index 3 allowed comparison with the results of Colgate and White (1964). The initial evolution of all three models ($10M_{\odot}$ polytropes of index 3), was identical, following the path ABC in Figure (4); consequently this part of the evolution will be discussed only once.

Figure (4) illustrates the history of one representative zone, ($M_r = 1.5M_{\odot}$) falling into the core, of the models just discussed. The contraction was initiated by introducing a

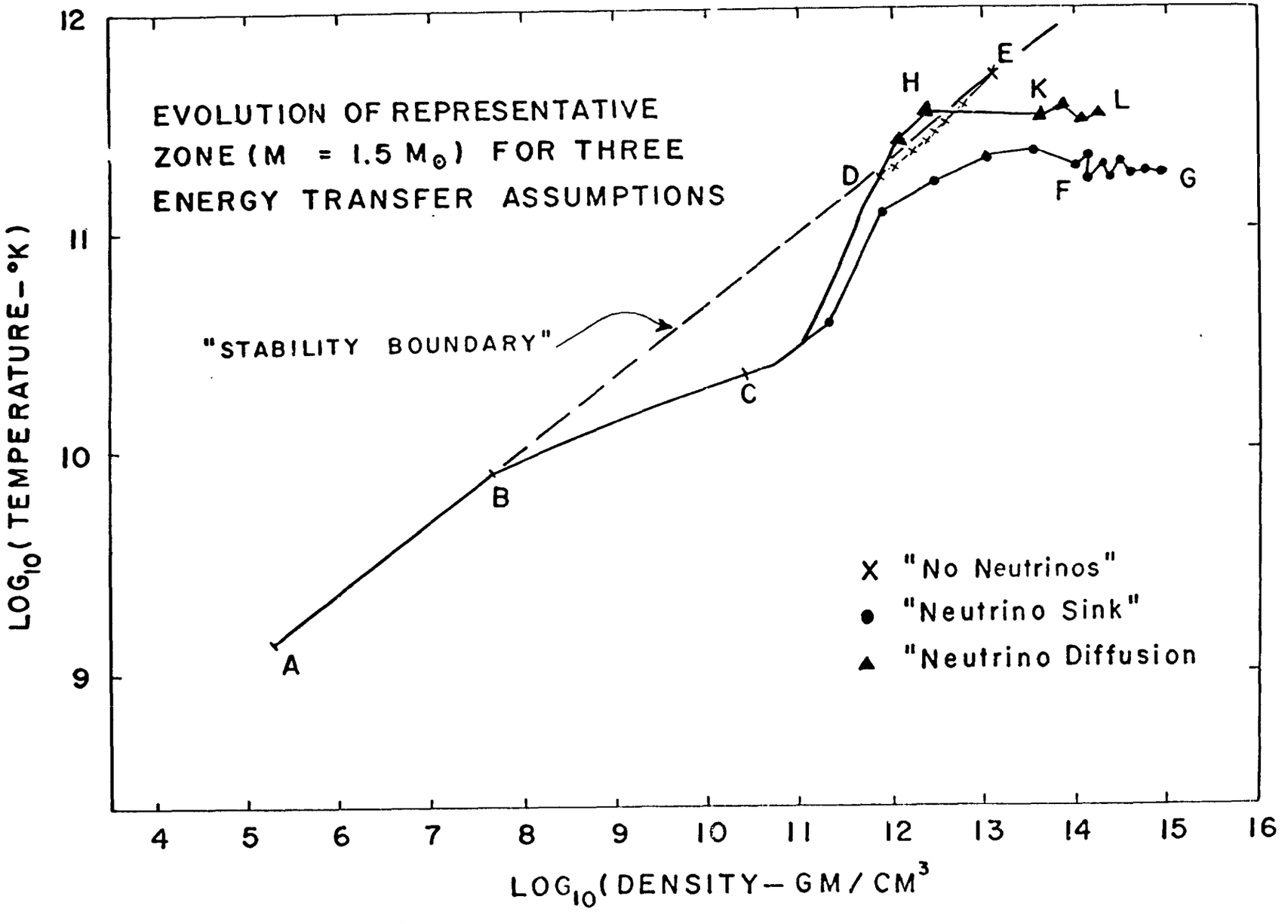
EVOLUTION OF REPRESENTATIVE
ZONE (M = 1.5 M⊙) FOR THREE
ENERGY TRANSFER ASSUMPTIONS
"STABILITY BOUNDARY"
A
B
C
D
E
F
G
H
K
L
X "No Neutrinos"
● "Neutrino Sink"
▲ "Neutrino Diffusion
LOG10 (TEMPERATURE – °K)
LOG10 (DENSITY – GM/CM3
12
11
10
9
4
5
6
7
8
9
10
11
12
13
14
15
16

small energy sink to evolve the model. This was done by uniformly increasing the combination pair-annihilation and plasmon neutrino rates throughout the model until it contracted to the collapse point, slow enough to follow a $\gamma = 4/3$ adiabat more or less, but fast enough to do so without using too much computing time. The stability condition (Appendix equation C. 1) on the hydrodynamic difference equations is unduly restrictive for the quasi-static evolution of hydrostatic models, so that this accelerated contraction was necessary. So long as the configuration follows the correct path in the pressure-temperature plane for pre-collapse, and at the point of collapse has negligible kinetic energy, this approximation is valid. This part of the evolution carried the zone along the path AB.

The evolution along the path BC represents the evolution of the material through the Fe-He phase change. At point B energy is removed by endoergic nuclear reactions so that the zones begin to fall inward rapidly. At point C the conversion of the iron-peak nuclei to helium and nucleons is nearly complete. In order to keep the amount of data manageable, quantities were printed out every 200 time cycles of the hydrodynamic calculation. The evolution was so rapid at this

point that the accurate position at which the transition was completed is not known, but it is probably as drawn in Figure (4).

1. "No-neutrino" model.

The evolution from C to D in Figure (4) may be explained as follows. The implosion proceeds until the nucleon terms in the equation of state provide sufficient pressure to halt the infalling material. When neutrino energy loss is neglected, the following artificial situation develops. When the electron Fermi energy rises sufficiently to cause inverse beta-decay, the number density of electrons does not rise much with an increase in density, and hence the pressure contribution due to electrons does not rise either. The free nucleons which are formed do contribute an ideal gas term to the pressure (in this model). Since neutrino energy loss is neglected in this model, the material falling upon the initial $0.5M_{\odot}$ core is shock-heated to high temperatures.

The path CD describes the thermodynamic history of the zone as it encounters this stationary core shock. The kinetic energy which the zone gained upon falling to this density was converted to thermal energy of an ideal nucleon gas. This may be seen from the following estimates:

Change in potential energy upon contraction	$\sim -5.3 \times 10^{52}$ ergs
Change in thermal energy necessary to support the core material hydrostatically	$\sim 4.2 \times 10^{52}$ "
Energy lost in photodisintegration of nuclei	$\sim 1.0 \times 10^{52}$ "
Energy left to form an over-pressure and mass ejection	$\lesssim 0.1 \times 10^{52}$ "

The energy available to form an overpressure is negligible as far as an explosion of the model is concerned. In fact the core continued to adjust itself as overlying layers continued to rain down, and the implosion was not reversed. During this period the zone plotted in Figure (4) evolved along path DE. The calculation was terminated when a core of about three solar masses was formed; at this point there was no indication of any possibility of mass ejection. Although the histories of only "representative" zones are given in the Figures, statements of results (as here with the absence of mass ejection) are based on examination of the behavior of all zones in the model.

During a homologous contraction (or expansion) every mass zone of hydrostatic gas mass has its pressure related to its density by

$$P = P_o \left(\frac{\rho}{\rho_o}\right)^{4/3}$$

where P_o is the pressure and ρ_o the density of this zone for some reference configuration. This relationship defines the path in the pressure-density plane upon which the mass zone must lie for hydrostatic configurations (which are homologous to the reference configuration). When the gravitational acceleration

$$g(r) = - \frac{G M (r)}{r^2}$$

is linear in the radius r, a gas sphere in free-fall contracts homologously. This occurs when

$$M(r) \sim r^3$$

or equivalently, when the density is constant.

$$\rho = \text{constant}.$$

For a density which decreases with radius, the outer zones of the gas sphere must be accelerated less than would be necessary for homologous contraction, and "left behind". The innermost zones of a gas cloud freely falling under its own gravity tend to fall homologously, leaving behind those zones which do not. Thus the relation $P \sim \rho^{4/3}$ defines a locus of hydrostatic configurations for the imploding core (and for the whole star model in so far as the homology requirement is satisfied). This curve in the P-ρ plane, and its corresponding curve in the ρ-T plane, define a sort of

stability boundary, such that if the pressure predicted by this relation is greater than the model actually has for a given density, ther the core is unstable toward contraction and cannot be static. The dashed line in Figure (4) defines such a boundary. Note that the evolutionary path of the "no-neutrino" model does not cross this line, although at point E the zone shown is a part of a quasi-static core of $3M_{\odot}$ and the stability boundary is approached. By this time the structure of the core is by no means a scaled-down version of the structure of the same matter in the initial hydrostatic model. Although the homology requirement for the use of the stability boundary is violated, in fact there is no evidence that any significant reversal of implosion or mass ejection is likely. For smaller mass cores, it will be seen that the stability boundary concept is useful.

2. "Neutrino Sink" Model.

The"neutrino sink" model differs from the "no-neutrino" model just described through the inclusion of an energy loss rate of the form:

$$Q = - 4.3 \times 10^{15} \frac{(T_9)^9}{\rho} - 1.1 (T_9^3) \rho \text{ erg/gm/sec}$$

This is the sum of approximate forms for electron pair-annihilation and plasmon decay neutrino loss processes

mentioned earlier. It is not maintained that this expression is the correct form to use. Quite the contrary, other processes such as the URCA process for nucleons are probably more important. What is important is that the neutrino energy production rate is almost certainly as large as this. If it is assumed arbitrarily that all neutrinos, once formed, escape from the model, then this energy loss rate is a lower limit.

What is the purpose of such an artificial model? Simply this: it shows that for this comparatively mild energy loss rate, there is no reversal of implosion, no mass ejection, but just the accumulation of a degenerate core of ever-increasing size when neutrino diffusion is neglected. This is shown in Figure (4), where this "neutrino sink" model follows the path CFG. In the segment CF the graphed zone encounters a stationary core shock, in which the infalling zones are slowed and become part of the core. For this model, the neutrino energy loss rate keeps the temperature much lower than was the case for the "no-neutrino" model. This causes the core to form at a much higher density than was the case in the "no-neutrino" model. This means that more gravitational potential energy has been released, but is

lost from the star. The continued loss of energy allows the core to evolve slowly to higher densities, along the path FG. The irregularities in the path along FG correspond to oscillations* of the core, perturbed by the continued infall of matter. The matter is quite degenerate at this point, so that temperature has little effect on the equation of state. Notice that the evolutionary path CFG never comes near the "stability boundary".

3. "Neutrino Diffusion" Model.

Neutrino opacity and the approximations involved in the assumption of diffusive energy transfer have been discussed. In this model the possibility of energy transfer by the diffusion of neutrinos is considered. It should be emphasized that the neutrinos were assumed to be in thermal equilibrium with the other particles in order to avoid a kinematic calculation.

The temperatures shown in Figure (4) are unreasonably high because of the approximate nature of the equation of state. In particular, the thermal contribution of the nucleons to the pressure was underestimated. The neutrino opacity depends sensitively upon the average neutrino energy,

---

* These oscillations may be due to the finite size of the mass zones as well as to the excitation of actual physical oscillations.

which depends upon the temperature. Because of this overestimate of the temperature, the collapse of a model using the electron-neutrino scattering opacity behaved much like the previously discussed "no-neutrino" model, that is, a hot core was formed, but there was no mass ejection. In order to examine the effects of neutrino energy transfer, the opacity in the core was kept low enough so that the energy transfer time scale was of the order of the hydrodynamic time scale. This affects only the zones of higher density,

$$\rho \gtrsim 10^{12} \text{ gm/cm}^3$$

so that opacity in the crucial region in which the infall of the matter is reversed, is just that for neutrino-electron scattering, with average neutrino energy $E \sim 3kT$. A report on investigation of the validity of this assumption for the opacity at high densities is currently being prepared for publication.

The "neutrino diffusion" model was calculated in exactly the same manner as the "neutrino sink" model until the neutrino mean free path became short compared with the dimension of the star. At this point the transfer of energy by neutrino diffusion was calculated, and some results are indicated in Figure (4). The path CD is identical with the

"no-neutrino" case, but the temperature continues to rise rapidly as DH shows.

That this shock heating is more pronounced than in the "no-neutrino" model is quite important. Why this is the case may be seen as follows. Neutrino diffusion removes energy from the core. Before the neutrino diffusion is initiated, neutrinos are unhindered as they escape the core, again removing energy. This loss of energy prevents the temperature from rising rapidly, so that it is nucleon degeneracy pressure rather than thermal pressure which halts the infall of the core. This means that the core will have a much greater density than in the case of the "no-neutrino" model, which in turn implies that more potential energy is released by the contraction. Hence more energy is available for expelling matter.

The situation is now unstable in the following sense. If the infalling matter supplies kinetic energy to the core faster than this energy can be removed by neutrino diffusion, the temperature will rise. Because the neutrino interaction cross-sections are roughly proportional to the square of the neutrino energy, and because at higher temperatures neutrinos are formed with higher energies, the opacity

increases. The transfer of energy by neutrinos then decreases, and the temperature rises still more. Thus the medium may become opaque if the inflow of kinetic energy is sufficiently high.

The greater potential energy released in the "neutrino diffusion" model is now available for reversing the implosion of the outer layers. A neutrino diffusion wave sweeps out of the core, leaving the matter behind it opaque. The zone shown in Figure (4) is heated so that the path DH lies well above the stability boundary. Along the path HKL, this zone falls into the core. The path KL shows the core adjusting itself while overlying matter is ejected. Figure (5) shows the curve already shown on Figure (4) as CDHKL but is now labeled MNOP. The new curve on Figure (5), DEF, corresponds to the zone with an interior mass

$$M_r = 2.0\ M_\odot$$

and which is ejected from the star. The path DE corresponds to the heating of the zone by the neutrino diffusion shock wave, and EF is the subsequent expansion of the zone as it leaves the star. The remnant core mass was 1.8 $M_\odot$.

C. Comparison With the Results of Colgate and White.

Although the hydrodynamics of supernova envelopes has

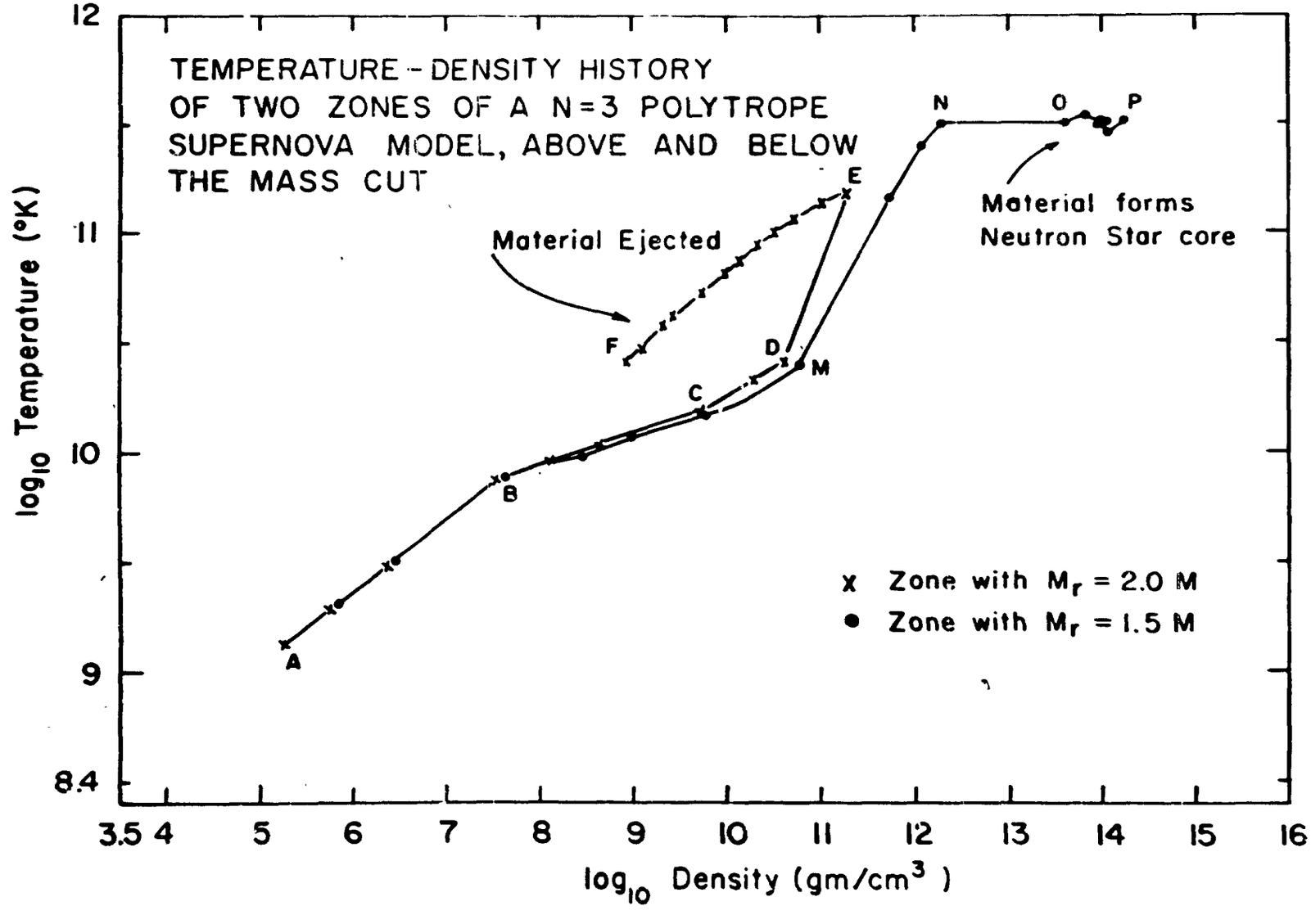
TEMPERATURE - DENSITY HISTORY
OF TWO ZONES OF A N=3 POLYTROPE
SUPERNOVA MODEL, ABOVE AND BELOW
THE MASS CUT
Material Ejected
Material forms
Neutron Star core
A
B
C
D
E
F
M
N
O
P
x Zone with M_r = 2.0 M
• Zone with M_r = 1.5 M
$\log_{10}$ Temperature (°K)
$\log_{10}$ Density (gm/cm^3)
12
11
10
9
8.4
3.5 4 5 6 7 8 9 10 11 12 13 14 15 16

received much attention, the only previously published investigations (of which the author is aware) of the initial instability and subsequent dynamical history of supernova interiors are those of Colgate and his collaborators. A review of these investigations by Colgate and White (1964) describes some of their more recent results and is the primary source for the following description of their work. In particular, the evolution of type II supernova models was followed by means of a numerical hydrodynamic computer code from the onset of gravitational collapse to the reversal of the infall of the core (due to terms in the equation of state corresponding to a nucleon hard-core potential). The loss of neutrinos emitted in inverse beta-decays cools the core during implosion. This loss rate is approximated by a simple analytic form; a more exact analysis would involve the evaluation of Fermi-Dirac integrals because the material becomes degenerate. A partial deposition of this neutrino flux in the stellar envelope and the shock wave reflected upon the formation of a neutron star core provide sufficient energy to eject ~ 80% of the mass of a 10 solar mass star. To simulate the emission and deposition of neutrinos from the shock wave formed by the infalling material raining

down upon the quasi-static core, half of the emitted energy was deposited in the matter external to the core shock. This deposition was initiated only when the core shock was formed and was turned off when the rarefaction due to expansion terminated the core shock. The time-dependent energy sink term, integrated over the core, is

$$\dot{s} = \int_o^M \left(\frac{dE_\nu}{dt} \right) dM$$

where the factor in parenthesis is just an analytic approximation to the inverse beta-decay neutrino loss rate, i.e.

$$\frac{dE_\nu}{dt} = - 0.1 \; T \; \rho^{5/3} \text{ erg/gm/sec}$$

where ρ is the density in grams/cm^3 and T the temperature in KeV. The rate of neutrino energy deposition that was used, in units of ergs/gm/sec, is

$$\left(\frac{dE_\nu}{dt}\right)_{\text{deposited}} = \frac{\dot{s}K}{4\pi r^2} \exp\left(-K \int_{r_{\text{shock}}}^{r} \rho \, dr\right)$$

for

$$r \geq r_{\text{shock}}$$

and where

$$K = \ln 2 / \left(\int_{r_{\text{shock}}}^{\infty} \rho \, dr \right.$$

The test for initial equilibrium proceeded for a real time of 30 seconds for a $10M_{\odot}$ polytrope of index 3 taken to be the model of a pre-supernova star. This model was inspired by considerations of Fowler and Hoyle (1964). The instability was initiated by removing 1% of the internal energy. The core formed cold with 5% of the mass of the star; after the implosion was reversed in the innermost mass zones a shock formed and neutrino deposition of energy was initiated. In this case $2M_{\odot}$ accumulated in the core before sufficient heat was deposited to reverse the implosion of the outer layers and create an explosion.

Colgate and White (1964) also discuss some calculations involving initial models of 2.0 and 1.5 solar masses. These models evolved on such a low adiabat that, rather than pass through Fe-He phase transition, they were brought to dynamic implosion by rapid electron capture (inverse beta-decay) at a density above $2 \times 10^{1-}$ gm/cm^3. The subsequent core formation, shock wave, neutrino emission and deposition, and finally explosion followed as in the $10M_{\odot}$ case. The expansion velocities and residual core mass were lower, but not drastically so.

Figure (6) compares the result of the "neutrino diffusion"

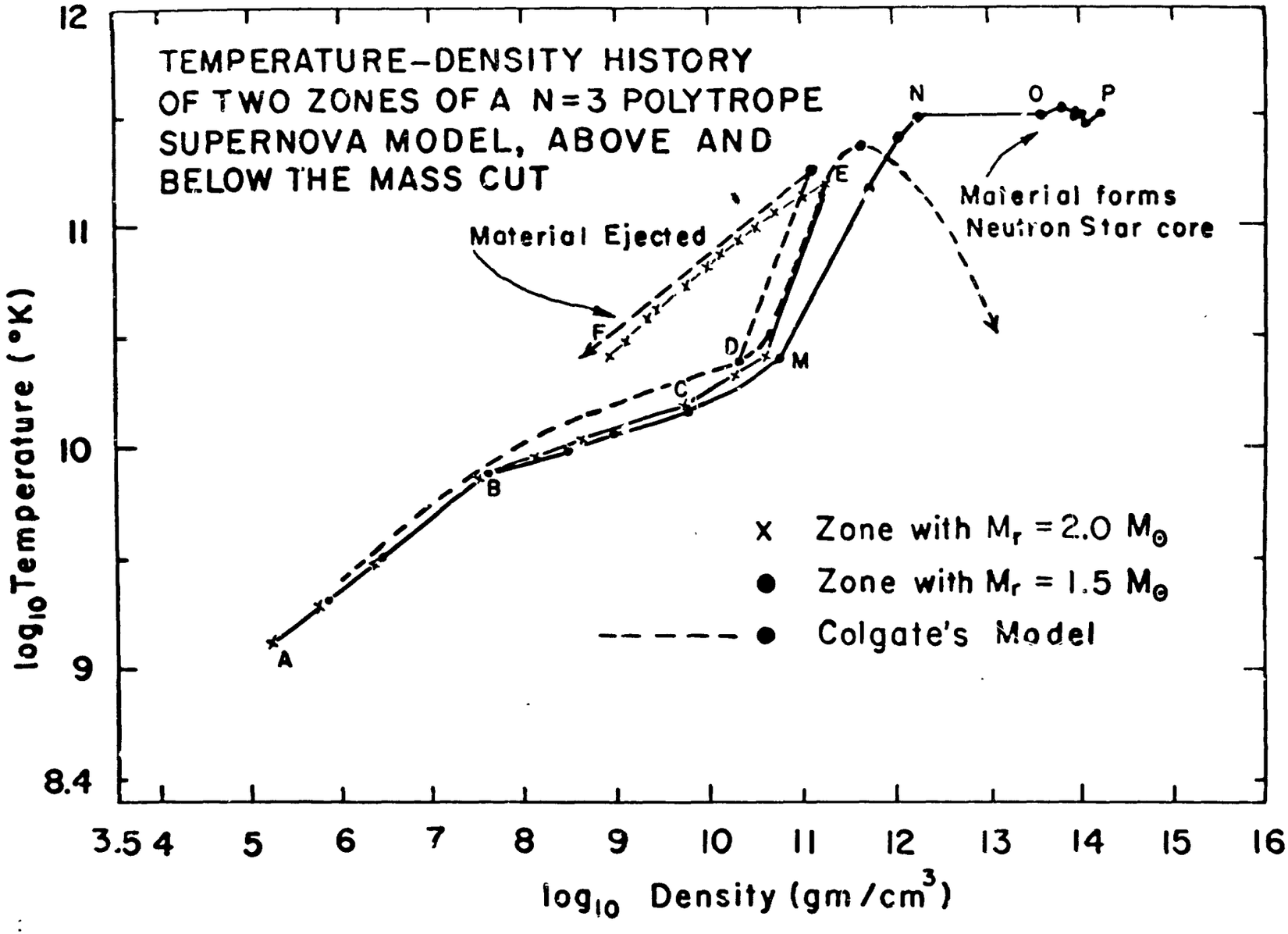
TEMPERATURE–DENSITY HISTORY
OF TWO ZONES OF A N=3 POLYTROPE
SUPERNOVA MODEL, ABOVE AND
BELOW THE MASS CUT
Material Ejected
Material forms
Neutron Star core
A
B
C
D
E
F
M
N
O
P
x Zone with $M_r = 2.0\ M_\odot$
● Zone with $M_r = 1.5\ M_\odot$
Colgate's Model
$\log_{10}$ Temperature (°K)
$\log_{10}$ Density (gm/cm^3)
12
11
10
9
8.4
3.5 4 5 6 7 8 9 10 11 12 13 14 15 16

model to the results of Colgate and White (1964). Although the data for the plot of Colgate's model were taken somewhat crudely from graphs, there seem to be three differences. This first concerns the Fe-He phase change region BCD which lies on a lower curve for the diffusion model. This does not affect the dynamics much since both models are in free-fall at this point. Considering the widely different methods used in treating this phenomenon, the difference in the two paths is not surprising. The second point is that Colgate's sudden heating (path DE and MN in the diffusion model) seems to occur at lower densities. This is thought to be attributable to Colgate's technique of depositing energy. The last difference is the rapid cooling of the core as shown by Colgate's model. Colgate's energy transfer technique probably is inaccurate at this point; this cooling occurs after the mass ejection so that its effect upon other aspects of the supernova phenomena is small. Also, the diffusion approximation will incorrectly predict the energy loss rate as the distribution function for neutrinos departs from its form for thermal equilibrium. The problem of core cooling would be properly handled only by a detailed transfer calculation.

D. Effect of Pre-collapse Structure.

Figure (7) illustrates the history of two representative zones of the centrally-condensed pre-supernova model described previously. This model was evolved slowly along a path

$$\rho \sim T^3$$

until electron capture instigated collapse. This phase, similar to the evolution of the $10M_\odot$ polytrope model before the Fe-He phase transition, is shown in Figure (7) as the paths AB and MN. By the time these zones had reached the vicinity of points B and N, the core had "bounced" and the neutrino diffusion wave was moving outward.

The effect of this diffusion "wave" may be seen in Figure (7). Consider the zone with 0.98 $M_\odot$ underneath it first. Along path NP there is a wiggle which was caused by initiating the diffusion calculation and has no significance. During this time the diffusion wave has not yet reached the zone. Path PQ shows the heating of this zone as it, falling in, encounters the diffusion wave sweeping outward. During the time the zone moves from Q to R it is inside the neutrino emitting surface. It falls on the core at point R, and evolves slowly from this point on. Further evolution is due to "slow" energy loss by neutrino diffusion (the time

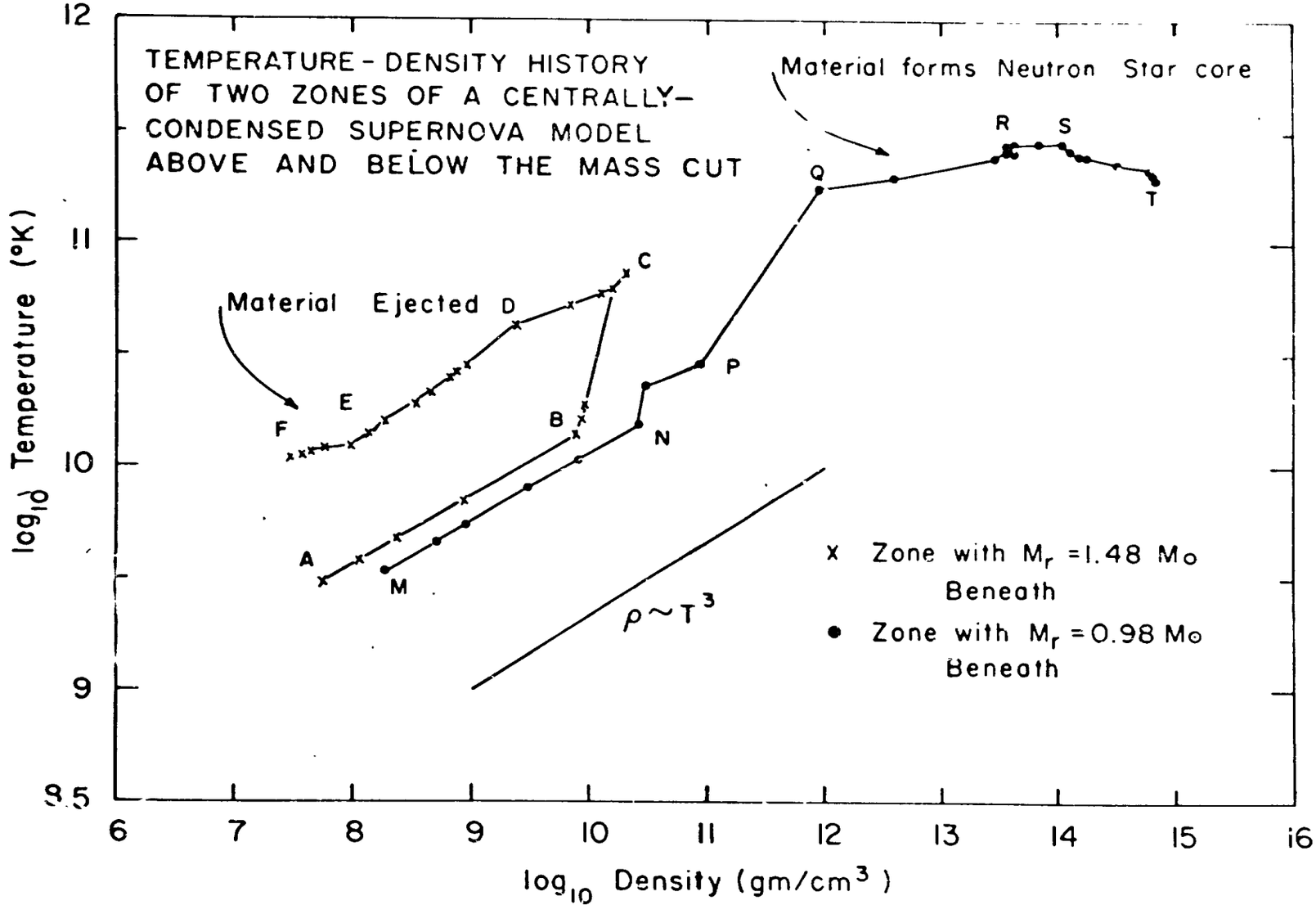
TEMPERATURE - DENSITY HISTORY
OF TWO ZONES OF A CENTRALLY-
CONDENSED SUPERNOVA MODEL
ABOVE AND BELOW THE MASS CUT
Material forms Neutron Star core
Material Ejected
A
B
C
D
E
F
M
N
P
Q
R
S
T
$\rho \sim T^3$
x Zone with M_r = 1.48 Mo Beneath
• Zone with M_r = 0.98 Mo Beneath
$\log_{10}$ Temperature (°K)
$\log_{10}$ Density (gm/cm^3)
12
11
10
9
9.5
6
7
8
9
10
11
12
13
14
15
16

involved between R and T is $t \geq 10^{-3}$ sec).

The ejected zone ($M_r = 1.48\ M_\odot$) encounters a combination of shock heating and neutrino diffusive heating along the path BC. At C, the peak temperature for this zone, expansion begins. Along CD there is some heating due to acceleration of lower zones, but along path DE the pair-annihilation neutrino energy losses make the path slightly steeper than $\rho \sim T^3$. At point E, the thermally decomposed nuclei begin to recombine by exoergic reactions. This causes the temperature to drop off more slowly along path EF. At this point the calculation was terminated.

The similarities and differences in the two structurally different models are summarized in Table I. The "velocity of ejected matter" quoted in Table I means the average velocity of that matter behind the ejection shock wave at the conclusion of the calculation. The velocity corresponding to the observed expansion velocities of supernova remnants should be less because an envelope of several solar masses still lies outside the ejection shock. Extension of these calculations to this asymptotic ejection velocity is contemplated.

The more violent ejection of matter from the centrally

condensed model is to some extent due to nuclear recombination late* in the expansion. The similarities are more striking than the differences. These two widely differing models, brought to collapse by different mechanisms, nevertheless have surprisingly similar characteristics. The remnant core mass seems to be higher for the less condensed model; this might be expected because the mass of the sphere inside which the gravitational acceleration,

$$g(r) = \frac{GM(r)}{r^2}$$

is nearly linear, is smaller in the more condensed model. This determines the mass of the material which halts its contraction as a unit; this material collapses approximately as a uniform density sphere would.

E. Comparison of Calculations and Observations.

Because of the low frequency of occurrence of supernova outbursts (about 1/century/galaxy) observational information is meager. Zwicky (1956) gives a history of supernova observations. More recent accounts by Shklovski (1960) and Minkowski (1964) make it reasonable to identify type II supernovae with the catastrophic disintegration of a massive

---

* The polytrope model was not followed this far.

star ($M>>M_{\odot}$). Table II contains a summary of some characteristic properties of supernovae type II. Details concerning the optical spectra and light curves, which are not investigated here, may be found in the references mentioned above.

Comparing Tables I and II, it will be seen that there is reasonable agreement between the observational evidence and theoretical predictions. The visual magnitude expected from the theoretical models has not been estimated, but the kinetic energy of ejected mass is appropriate. The velocity of ejection appears larger than observed, but in fact the asymptotic value of the velocity will be lower, especially if the star has an extensive envelope as has been assumed. This comment applies to the condensed model, in particular, which is envisaged as having a large envelope.

IV. Interpretation of the Results of the Model Calculations.

A. Peak Temperature and Muon Neutrino Energy Loss. Muon neutrinos do not have the same interaction cross-sections as electron neutrinos. Unfortunately the opacity for mu neutrinos in a hot, dense medium like a supernova core is not as well investigated as for electron neutrinos. It appears that neutrino production by muon-pair annihilation will dominate production from simple muon decay, for higher temperatures at least, as will be shown by the following argument.

Some rough estimates of the muon neutrino energy loss rates may be made as follows. The number density of fermion pairs,

neglecting any decay modes, is given by

$$N = \frac{2}{h^3} \int_0^\infty \frac{d^3 p_\pm}{1 + \exp\left[(\varepsilon_\pm \pm \mu)/kT\right]}$$

Assume that the muons are nondegenerate and that the number densities of μ_+ and μ_- are equal. Then, since*

$$\exp\left[(\varepsilon_\pm \pm \mu)/kt\right] >> 1$$

where the maximum of the integrand occurs, then

$$N_p = \left(\frac{mc}{\hbar}\right)^3 \frac{1}{\pi^2} f(\beta)$$

where N_p is the number density of muon pairs, mc^2 is the rest energy of the muon, and

$$f(\beta) = \int_0^\infty \exp\left[-\beta(1+x^2)^{1/2}\right] x^2 \, dx$$

$$\beta = \frac{mc^2}{kT} .$$

For large β, that is, $kT << mc^2$,

$$f(\beta) \approx \sqrt{\pi}/2 \; \frac{e^{-\beta}}{\beta^{3/2}}$$

so that

$$N_p \sim \frac{10^{38}}{3.2} \; \frac{e^{-\beta}}{\beta^{3/2}}$$

The rate of neutrino energy loss at high enough temperatures by muon decay is roughly

$$\dot{s} \sim - 2N_p \, \bar{\varepsilon}/(\rho\tau) \text{ erg/gm/sec}$$

---

* Chiu and Stabler (1961) present this approximation for electrons.

where $\bar{\epsilon}$ is some average energy of the emitted neutrino, ρ the matter density, and τ the half life of the muon. Assuming equipartition of energy, $\bar{\epsilon}$ might be of the order of 35 MeV.

Using the same approximations of nondegeneracy and $kT << mc^2$, Chiu and Stabler give the approximate pair annihilation energy loss rate

$$\dot{s}_e = - 4.8 \times 10^{18} \frac{T_9^3}{\rho} e^{-(2m_e c^2/kT)} \quad \text{ergs/gm/sec}$$

Correcting this for the heavier mass muon,

$$\dot{s}_\mu \approx \left(\frac{m_\mu}{m_e}\right)^9 \dot{s}_e$$

$$\approx 3 \times 10^{32} \frac{T_9^3}{\rho} e^{-(2400/T_9)}$$

Neglecting the effect of muon decay on the number of muon pairs formed in equilibrium with radiation may be justified as follows. The characteristic time for muon deacy is 2×10^{-6} seconds. Taking $kT << m_\mu c^2$ the muon pair annihilation cross-section has roughly the same magnitude as

$$\sigma \sim \frac{8\pi}{3} \left(\frac{e^2}{m_\mu c^2}\right)$$

$$\sim 10^{-29} \text{ cm}^2$$

So that the mean reaction time is

$$\tau_r \sim \frac{1}{N \sigma v}$$

which for $T_9 = 120$ gives

$$\tau_r \sim 10^{-13} \text{ sec}$$

so that

$$\tau_r << \tau \text{ decay}$$

and this implies that muon decay does not greatly alter the muon number density. Some estimates for the energy loss rates by muon type neutrinos are given in Table III.

The energy loss rates have units erg/gm/sec and are all evaluated at a density of 10^{12} gm/cm^3. The relaxation times for these rates, if they proceed unimpeded are given in Table IV.

In the last case the energy loss by neutrinos emitted by muon decay is dominant, but the time scale for cooling is then longer than the characteristic collapse and mass ejection time scale. From these rough estimates it might be expected that the temperatures for the n=3 polytrope model, Figure (5), are artificially high. The muon-neutrino energy loss is probably not so large for the isothermal model. It is not convincing to estimate what effect muon neutrinos will play in supernova explosions without a careful analysis of all possible reactions, both for neutrino production and neutrino opacity, and a careful estimate of the temperature. It does appear that larger remnant cores might be expected with the inclusion of muon-type neutrino energy loss, but little more can be said at this time.

B. Electron Neutrino Luminosity and Detectability. The immense energy radiated by neutrinos that the previous models predict, and the high temperature of the emission surface, suggest that it might be possible to detect supernovas by their neutrino flux. Dr. Raymond Davis, Jr.* of

---

* R. Davis, Jr. (1965).

Brookhaven has kindly provided information about his detector with which to evaluate this possibility.

If a detector contains N absorbers, then the fraction of the total integrated neutrino flux absorbed in the detector is

$$f = \frac{N\sigma}{4\pi R^2}$$

where σ is the interaction cross-section and R is the distance of the source. The total integrated flux is roughly

$$F = \frac{E_{tot.}}{3kT}.$$

where $E_{tot.}$ is the total energy emitted in the form of neutrinos (only electron neutrinos are considered because of the uncertainty in the muon reaction rates), and T is the temperature of the zone just inside the neutrino emission surface.

For kT ~ 10 MeV, and

$$E_{tot.} \sim 10^{53} \text{ ergs}$$

$$N \sim 2 \times 10^{30} \ Cl^{37} \text{ atoms}$$

$$\sigma \sim 7 \times 10^{-41} \text{ cm}^2,$$

where the cross-section is for the reaction

$$\nu + Cl^{37} = e^- + A^{37},$$

and for a minimum detectable signal of 100 counts,

$$R \sim 1.5 \times 10^{22} \text{ cm}$$

$$\sim 5 \text{ kpc.}$$

the maximum source distance is 5 kiloparsecs. According to Allen*, the diameter of the Galaxy is

$$D \sim 25 \text{ kpc.}$$

Recalling the supernova rate quoted earlier, one per century per galaxy, it appears that no burst of electron neutrinos is likely to have produced a detectable signal since suitable detectors have been operating.

C. General Relativity and Core Collapse.

In order to check the neglect of general relativity, the Schwarzschild radius

$$r_s = \frac{2\,GM}{c^2} \approx 0.3 \times 10^6 \left(\frac{M}{M_\odot}\right) \text{cm.}$$

is compared to the radius of the dense core.

	Condensed Model	n = 3 polytrope model
r_s/r core	0.22	0.38

As anticipated the general relativistic effects are becoming important, especially for the n = 3 polytrope model. These effects will be more pronounced in the core. The mass ejection, occurring before such high densities are reached

---

* Allen (1963), p. 267.

(r_s/r_{core} for the n = 3 polytrope is then only ~ 0.16), will be less sensitive to this effect. However, the bounce point for the core collapse, where the infall is halted, is somewhat dependent on both the nuclear equation of state and the temperature of the infalling matter. Careful investigation with general relativistic hydrodynamic equations is needed to confirm that neglect of general relativity is reasonable until after mass ejection.

V. Critique of Calculational Method.

Approximating the transfer of energy by neutrinos by a model of diffusing neutrinos in local thermodynamic equilibrium is probably correct in a rough sense, but while it may be on firmer theoretical ground than the intuitive approach of Colgate and White (1964), it leaves much to be desired. On the other hand, the solution of a transport equation coupled with hydrodynamic motion poses extremely difficult computational problems.

The shock width in Figure (5), path MN, and in Figure (7), path PQ, stretches over a density range of more than a power of ten. Direct examination of the numerical results of the calculation reveal that in general the width of the shock zone is smeared over too wide a

region due to the lack of an adequately fine zoning mesh. Unfortunately, the present generation of computers is too slow to make the use of models with more zones feasible. The computing time goes as the square of the number of mass zones in the model, so that this limitation is difficult to overcome.

By the similarity in energy release and core size as obtained by the polytrope of index 3 and the isothermal model, it appears that the interior dynamics of supernova are relatively insensitive to the structure of the pre-supernova model. This does not mean that the existence of an extensive envelope such as found in massive red giants might not affect the velocity of ejection and the peak shock temperature in the matter ejected. It does mean that the implosion and "bounce" of the core, as well as the neutrino energy transfer process are insensitive to initial structure. The interior dynamics is much the same for the two models presented.

Summary

The calculations reported here indicate that it is possible to construct reasonable models of supernova by assuming energy to transferred by electron-type neutrinos during stellar collapse. Whether or not considerable mass

ejection by this process actually occurs depends critically upon the average neutrino energy and the opacity for neutrinos in regions of high density ($\rho \geq 10^{12}$ gm/cm^3). Unfortunately these quantities remain uncertain. Because of the temperature uncertainty, the emission rate of muon-type neutrinos is also unknown. Even the relatively low estimates of energy loss rates made for muon-decay (neutrinos from pion-decay may be more important) indicate that muon-type neutrino processes will be of paramount importance at the higher temperatures.

Appendix on Numerical Methods

Because the techniques used in this research are not as yet well known to most physicists and astronomers, a brief summary is presented here. The equations of hydrodynamics may be written as follows:

1) mass conservation

$$dM_R = 4\pi R^2 \rho dR,$$

2) momentum conservation

$$\frac{dU}{dt} = -\frac{GM_R}{R^2} - 4\pi R^2 \frac{dP}{dM},$$

3) energy conservation

$$dE = \dot{s}\, dt - PdV,$$

but using

$$dE = \left(\frac{\partial E}{\partial V}\right)_T dV + \left(\frac{\partial E}{\partial T}\right)_V dT$$

gives

$$dT = \frac{1}{\left(\frac{\partial E}{\partial T}\right)_V} \left(\dot{s}\, dt - \left(P + \left(\frac{\partial E}{\partial V}\right)_T\right) dV\right),$$

4) equation of state as a function of temperature T and specific volume V

$$P = P(v,T),$$

$$\left(\frac{\partial E}{\partial T}\right)_V = ET(V,T),$$

$$\left(\frac{\partial E}{\partial V}\right)_T \equiv EV(V,T).$$

In these equations M_R is the mass interior to some radius R, $\rho = 1/V$ is the density, U is the velocity of Lagrangian mass element at R, E is the internal energy per unit mass, $\dot{s}$ the rate of addition of energy per unit mass, and P is the pressure.

A. Difference Equations. As they stand, the fluid dynamic equations are highly nonlinear. Because of this difficulty only a few analytic solutions are available, and all of rather limited applicability. For other cases one is usually forced to some sort of approximation technique which is often as complex as numerical solution, and which may tend to obscure the physical situation. Even the approximation techniques are generally restrictive. In view of these problems it is often the case that numerical solution difference equations is preferable. At first we neglect radiative transfer of energy. Neutrino energy transfer will be treated subsequently.

The star will be divided into concentric spherical shells by J boundaries numbered 1, 2, 3,...J (from the center outward). Quantities associated with the zone boundaries will be subscripted j; those associated with zone centers

are subscripted j + 1/2. Time centering is indicated by a superscript n in a like manner.

After using some simpler forms, difference equations quite similar to those of Colgate and White (1964) were adopted. Although they have been presented in the above reference, the equations are discussed here for completeness.

The initial configuration is input. The position and velocity of each boundary

$$R_j^1$$

$$j = 1, \ldots JJ$$

$$U_j^1$$

where JJ is the number of boundaries, the pressure, specific volume and temperature of each zone

$$P_{j+1/2}^1$$

$$V_{j+1/2}^1$$

$$T_{j+1/2}^1$$

must be specified. The mass of each zone may be calculated from

$$DM_{j+1/2}^1 = \frac{4\pi}{3}\left(R_{j+1}^1\right)^3 - \left(R_j^1\right)^3 / V_{j+1/2}^1 \qquad \text{A.1}$$

The effective mass of a zone as seen from a boundary is the simple average

$$DM_j^1 = \tfrac{1}{2}\left(DM_{j+1/2}^1 + DM_{j-1/2}^1\right)$$

A.2

which assumes that the zone masses differ little. In practice it was found that results were often better when neighboring zone masses were the same or changed by a small constant fraction. The total mass inside a boundary j+1 is

$$XM_{j+1}^1 = XM_j^1 + DM_{j+1/2}^1$$

A.3

In the Lagrangian system mass is necessarily conserved until the zoning is changed. When a system changes drastically it is sometimes possible to shorten the time required for a calculation by rezoning the configuration, but otherwise the zone masses remain the same.

The equation for momentum conservation may be written as

$$U_j^{n+1/2} = U_j^{n-1/2} - (R_j^n)^2\left[P_{j+1/2}^n - P_{j-1/2}^n + Q_{j+1/2}^{n-1/2} - Q_{j-1/2}^{n-1/2}\right]\Delta t^n/DM_j$$

A.4

$$- \frac{G\ XM_j}{(R_j^n)^2}\,\Delta t^n$$

where the fluid velocity is

$$U \equiv \frac{dR}{dt}$$

so

$$R_j^{n+1} = R_j^n + U_j^{n+1/2} \Delta t^{n+1/2}$$

A.5

From this the specific volume car be updated by

$$V_{j+1/2}^{n+1} = \frac{1}{3} \frac{(R_{j+1}^{n+1})^3 - (R_j^{n+1})^3}{DM_{j+1/2}}$$

A.6

which reflects mass conservation. The specific volume evaluated at the same point in time as the fluid velocity U, that is at n+1/2, will be useful.

$$V_{j+1/2}^{n+1/2} = \tfrac{1}{2} (V_{j+1/2}^{n+1} + V_{j+1/2}^{n})$$

A.7

At this point a linear extrapolation in time is made for the new temperature at point n+1/2. Initially

$$T_{j+1/2}^{3/2} = T_{j+1/2}^{1}$$

but afterward

$$T_{j+1/2}^{n+1/2} = T_{j+1/2}^{n} + \frac{1}{2} \frac{\Delta t^{n+1/2}}{\Delta t^{n-1/2}} (T_{j+1/2}^{n} - T_{j+1/2}^{n-1})$$

A.8

This will be used to determine the temperature at the epoch n+1.

Evaluating the equation of state at time step n+1/2 gives

$$P_{j+1/2}^{n+1/2} = P(T_{j+1/2}^{n+1/2}, \quad V_{j+1/2}^{n+1/2}),$$

A.9

$$\left(\frac{\partial E}{\partial T}\Big|_V\right)_{j+1/2}^{n+1/2} = ET\ (T_{j+1/2}^{n+1/2}, \quad V_{j+1/2}^{n+1/2}),$$

A.10

$$\left(\frac{\partial E}{\partial V}\Big|_T\right)_{j+1/2}^{n+1/2} = EV\ \ (T_{j+1/2}^{n+1/2}, \quad V_{j+1/2}^{n+1/2}).$$

A.11

The quantity Q in the momentum conservation difference equation is the so-called pseudo-viscosity term which stabilizes this set of difference equations. When zone boundaries approach rapidly it supplies a large pressure to prevent them from crossing. In a shock the pseudo-viscosity term converts kinetic energy of zone motion into thermal energy, and is negligible elsewhere. The form used is

$$Q_{j+1/2}^{n+1/2} = 2\ (U_{j+1}^{N+1/2} - U_j^{n+1/2})/V_{j+1/2}^{n+1/2} \quad \text{if} \quad V_{j+1/2}^{n+1} < V_{j+1/2}^{n}$$

$$\text{and } U_{j+1}^{n+1/2} < U_j^{n+1/2}$$

$$= 0 \quad \text{otherwise,}$$

A.12

which is zero on expansion.

The energy conservation equation becomes

$$T^{n+1}_{j+1/2} = T^{n}_{j+1/2} + \frac{1}{ET^{n+1/2}_{j+1/2}} \left[- (P^{n+1/2}_{j+1/2} + Q^{n+1/2}_{j+1/2} + EV^{n+1/2}_{J+1/2}) \right.$$

$$\left. * \ (V^{n+1}_{j+1/2} - V^{n}_{j+1/2}) + \dot{s}^{n+1/2}_{j+1/2} \ \Delta t^{n+1/2} \right]$$

A.13

Although the energy source term $\dot{s}$ has not been specified, a form for it could have been evaluated at epoch n+1/2 along with (A.9) for instance.

B. Pseudo-viscosity Technique. The pseudo-viscosity technique for treating hydrodynamic shocks is due to Von Neumann and Richtmyer (1950). There are few* references to it in the literature although it seems to be arousing some interest among astrophysicists.

Attempts to solve the equations of fluid motion by numerical procedures are greatly complicated by the presence of shocks. Mathematically the shocks are represented by surfaces upon which the temperature, density, pressure and fluid velocity are discontinous. The partial differential equations governing the motion require boundary conditions connecting the values of

* The author found Richtmyer (1957), Fromm (1961), Henyey (1959), Christy (1964) and Colgate and White (1964) most useful.

these quantities on each side of the shock surface. The Rankine-Hugoniot relations, i.e., local conservation of mass, momentum and energy by the fluid, supply the necessary restrictions, but are difficult to apply during a calculation because the shock surface moves relative to the mesh points in space-time which are used for the numerical work. The nonlinearity of both the differential equations and the boundary conditions does not simplify the problem. The motion of the shock surfaces is not known in advance but is determined by the differential equations and the boundary conditions themselves.

The method of Von Neumann and Richtmyer automatically treats shocks and avoids the necessity for pre-knowledge of shock motion by utilizing the effects dissipative mechanisms (such as radiation, viscosity, and heat condiction) upon shocks. When viscosity is considered, the mathematical shock discontinuity becomes a thin layer in which the pressure, density, fluid velocity and temperature vary rapidly but continuously. By introducing an artificial dissipative mechanism to spread this shock layer over a few mesh points, the difference equations approximating the equations of fluid motion can be used throughout the calculation, as if no shocks were present.

In the numerical results the shocks appear as rapid changes in the variables, almost discontinuities, which have very nearly the correct speed and across which the pressure, temperature, and density have very nearly the correct changes.

In an actual physical problem the dissipative mechanisms are generally much smaller than the artificially introduced viscosity term. The limit on computational reproduction of a physical situation is that the zone size be smaller than the smallest dimension of interest. The quadratic dependence of (Q) on the velocity difference insures that this form for the artificial viscosity is small except in the shock region. Note that the 1/V dependence gives an increasing pseudo-viscosity for large compression.

C. Stability of the Difference Equations. For a more complete discussion of the stability of finite difference approximations the reader is referred to Von Neumann and Richtmyer (1950), Fromm (1961) and Richtmyer (1957). To clarify the meaning of stability, consider the exact solution $\Psi(r,t)$ to the one-dimensional differential equations of fluid dynamics for some specified initial-value problem. Let Ψ_j^n be the corresponding solution to a system of difference equations which approximate these differential equations

The error of the approximation is then

$$|\Psi_j^n - \Psi(r=j\Delta r,\ t=n_\Delta t)|$$

Suppose that this error is small enough at some time t, and consider some small perturbation $\delta\Psi$. Does this perturbation grow with time? If so the difference scheme is obviously unacceptable as an approximation to $\Psi(r,t)$.

The criterion for stability against such small perturbations, for a set of difference equations such as presented here, is that the time step for integration Δt satisfy

$$\Delta t < \frac{\Delta x_{j+1/2}}{v_s} \qquad \text{C.1}$$

where Δx is a zone width and v_s is the local sound velocity. This must be true for each zone. There is a simple physical interpretation for this restriction. Neglecting any sort of radiative transfer and considering only gasdynamic effects, the minimum time for material at zone boundary j to communicate with material at zone boundary j+1 is just the sound traversal time t_s

$$t_s = \frac{x_{j+1} - x_j}{v_s} = \frac{\Delta x_{j+1/2}}{v_s}$$

The requirement

$$\Delta t < t_s$$

is simply that conditions at boundary j+1, say, at time epoch n+1 be physically independent of what transpires at boundary j at the same epoch n+1. Most physicists are more familiar with the analagous situation in relativity where the velocity of light plays the part here taken by the sound velocity. Although such a restriction is mathematically required of difference equations such as these, this restriction is physically necessary only when gasdynamic motions having velocities of the order or greater than the sound velocity are encounteed. If this is not the case a different set of difference equations might be developed which had a less stringent requirement* on the integration time step.

For a complex problem in which there are drastic changes from the initial configuration, considerable computational time may be saved by choosing the integration time step Δt as the maximum value consistent with the stability requirement (C.1). In the supernova problem it was discovered that this requirement, while necessary, was not sufficient to reproduce the physical situation faithfully. In the adiabatic contraction of a gravitating uniform sphere, it was found that the analytic solution was not successfully

---

* See Henyey (1959) for example.

approximated unless some restriction like the following was used:

$$\Delta V^{n+1/2} \leq 0.02\ V^{n},$$

so that the fractional change in specific volume was only a few percent. Colgate and White (1964) use the following simple and effective restriction on the time interval.

$$\Delta t^{n+3/2} \leq \frac{0.02 * V^{n}_{j+1/2} * \Delta t^{n+1/2}}{|V^{n}_{j+1/2} - V^{n-1}_{j+1/2}|}$$

C.2

In the difference form for the energy equation, an energy source term $\dot{s}$ appears. This allows energy to be added or removed locally, although as written does not explicitly account for energy transfer between zones. When energy is suddenly added or lost instabilities often result. Now the energy density E of a fluid may be written as

$$E = \frac{1}{\gamma - 1}\ PV$$

where P is the pressure, V the specific volume, and γ the "ratio of specific heats" which is constant for an ideal gas. Generally γ is a slowly varying function. With this in mind, the following time interval restriction was used

$$\Delta t^{n+3/2} \leq \frac{0.02\ P^{n}_{j+1/2}\ V^{n}_{j+1/2}\ \Delta t^{n+1/2}}{|P^{n}_{j+1/2}\ V^{n}_{j+1/2} - P^{n-1}_{j+1/2}\ V^{n-1}_{j+1/2}|}$$

C.3

and found to be adequate.

Using these three restrictions on the time step, the new time interval can be calculated. The sound velocity was found to be adequately represented by the simple approximation

$$v_s \approx \sqrt{2PV}$$

The time intervals $\Delta t^{3/2}$ and $\Delta t^{1/2}$ are input. Then Δt^{n}, which is needed in (A.4), the momentum conservation equation, is

$$\Delta t^{n} = \frac{1}{2}\ (\Delta t^{n+1/2} + \Delta t^{n-1/2})$$

C.4

This procedure allows a small, conservative estimate of the time interval to be input which insures that the stability requirements are not violated. The scheme then chooses the optimum time interval and rapidly approaches it. It is noted in passing that the reason for centering these difference equations in time* is to allow this calculated time step scheme to be used accurately with varying time steps.

---

* Only the pseudo-viscosity Q in (A.13) is not centered in time, a condition mitigated by the fact that Q is not a physical but a computational quantity, and that computations using this Q are accurate.

D. Boundary Conditions. In the supernova problem the interior boundary was taken to be at the origin, so by symmetry

$$R_1^n = 0$$

$$U_1^n = 0$$

for all time. This was not necessary; the inner boundary could have been at some distance R from the center of the star, acting as a spherical piston with velocity

$$U_1^n = f(t^n)$$

which in general varies in time.* There are difficulties associated with zones near a piston in this sort of scheme, however, and care should be taken.

Having specified the center of the star as the inner boundary, symmetry assures that pressure, temperature and specific volume are continuous through the origin and no inner boundary condition need be specified. The outer boundary is free to move, however,

$$U_{JJ}^n \neq 0$$

in general, so that its motion will be determined by the pressure (and artificial viscous pressure) at JJ+1/2. These are not calculated and must be imposed. If

* Christy, R. (1964).

$$P^{n}_{JJ+1/2} = - P^{n}_{JJ-1/2}$$

$$Q^{n-1/2}_{JJ+1/2} = - Q^{n-1/2}_{JJ-1/2}$$

D.1

then the total calculational pressure (P+Q) will be zero at JJ. This boundary condition was used. In this particular problem the motion of the inner regions was most interesting so that the choice of surface boundary condition did not happen to be critical.

E. Analytic Checks of Numerical Results. In order to test the validity of the numerical techniques employed, several problems for which exact analytic solutions exist were calculated. Some of these results are to be found in Colgate and White (1964), and they are reproduced in the author's thesis both as an argument for the validity of these particular difference equations and because they provide insight into the technique. The problems for which checks were made are: (1) a strong, plane shock propagating through an ideal gas with $\gamma = 5/3$ and density decreasing with the -7/4 power of the distance, (2) a strong spherical blast wave in an ideal gas with a density

$$\rho \sim R^{-n},$$

(3) the adiabatic collapse of an ideal gas sphere of uniform density, and (4) the hydrodynamic motion (or lack of it) of a gravitating gas sphere in hydrostatic equilibrium.* There is excellent agreement between the numerical and analytical solutions in all four cases.

F. Radiative Energy Transfer. If the diffusion approximation is valid the change in energy density due to sources and time-dependence can only affect lengths large compared to the mean free path. Then, for conservation of energy,

$$\frac{\partial E}{\partial t} + v\nabla E = \dot{s} - \frac{1}{\rho} \nabla \cdot \vec{J}$$

where $\dot{s}$ is the energy generation rate (per unit mass) due to sources, E the energy density per unit mass, v the velocity of the source, ρ the mass density, and $\vec{J}$ the energy flux. If source motion can be neglected, and macroscopic changes occur on a time scale much larger than the mean free time for the diffusing particles, then

$$\rho\dot{s} = - \nabla \cdot (\frac{\lambda_c}{3} \frac{dE}{dT} \Delta T)$$

Assuming sperical symmetry, this may be rewritten as

$$D \frac{dT}{dR} = - \frac{L(r)}{4\pi R^2}$$

where r is the radial coordinate and

---

* The exact solutions for (1), (2) and (3) are to be found in Burgers (1949), Sedov (1959), and Colgate and White (1964), respectively.

$$L(R) = \int_0^r 4\pi R^2 \, \dot{s} \, \rho \, dR$$

$$D = \frac{\bar{\ell}_c}{3} \frac{dE}{dT}$$

which are the standard forms for radiative diffusion used in quasi-static stellar models.

If macroscopic changes occur fast enough so that work done by pressure forces PdV must be included in the energy conservation equation, then

$$dE = \dot{s} \, dt + \frac{1}{R^2 \rho} \frac{\partial}{\partial R} \left(R^2 \frac{\bar{\ell}_c}{3} \frac{\partial (aT^4)}{\partial R} \right) dt - PdV$$

where spherical symmetry is assumed, V is the specific volume and a is the radiation constant.* Using $dM = 4\pi\rho R^2 dR$,

$$dE = \left(\dot{s} - \frac{\partial L}{\partial M} \right) dt - PdV$$

where

$$L = - (4\pi R^2)^2 \frac{ac}{3\bar{k}} \frac{d(T^4)}{dM}$$

F.1

and

$$\bar{k} = \frac{1}{\rho \bar{\ell}}$$

F.2

is the Rosseland mean opacity. Rewriting the energy conservation equation in terms of the temperature T gives

$$dT = \left[\left(\dot{s} - \frac{\partial L}{\partial M} \right) dt - \left(P + \left. \frac{\partial E}{\partial V} \right|_T \right) dV \right] / \left(\left. \frac{\partial E}{\partial T} \right|_V \right),$$

F.3

* For electron-type neutrinos and antineutrinos in thermal equilibrium and in equal abundance, the radiation constant is a(neutrinos) $\approx \frac{7}{8}$ a(photons).

where $(\frac{\partial L}{\partial M})dt$ is the energy lost by diffusive transfer, PdV is the work extracted by macroscopic motion, and $\dot{s}$ is the energy gain by other mechanisms.

G. Difference Equations and Boundary Conditions For Radiative Transfer. Equations (F.1), (F.2) and (F.3) may be incorporated into the hydrodynamic difference equations discussed in the previous section. Comparing (F.3) with our earlier energy conservation equation suggests the following difference equation, by analogy with (A.13),

$$T_{j+1/2}^{n+1} = T_{j+1/2}^{n} + \frac{1}{ET_{j+1/2}^{n+1/2}} \Big[- (P_{j+1/2}^{n+1/2} + Q_{j+1/2}^{n+1/2} + EV_{j+1/2}^{n+1/2}) (V_{j+1/2}^{n+1} - V_{j+1/2}^{n}) + (\dot{s}_{j+1/2}^{n+1/2} - \frac{(AL_{j+1}^{n+1/2} - AL_{j}^{n+1/2})}{DM_{j+1/2}}) \Delta t^{n+1/2} \Big]$$

G.1

But then (F.1) becomes

$$AL_{j}^{n+1/2} = - \frac{16\pi^2 ac}{3} (R_{j}^{n+1/2})^4 \frac{(T_{j+1/2}^{n+1/2})^4 - (T_{j-1/2}^{n+1/2})^4}{(DM * AK)_{j}^{n+1/2}}$$

G.2

where

$$(DM * AK)_{j}^{n+1/2} = \frac{1}{2} (DM_{j+1/2} AK_{j+1/2}^{n+1/2} + DM_{j-1/2} AK_{j-1/2}^{n+1/2})$$

G.3

and (F.2) becomes

$$AK_{j+1/2}^{n+1/2} = AK\ (T_{j+1/2}^{n+1/2},\ V_{j+1/2}^{n+1/2})$$

G.4

The term $AL_{j+1}^{n+1/2}$ involves quantities evaluated at space points j-1/2, j. and j+1/2. The latter will not have been evaluated when $T_{j+1/2}^{n+1}$ is to be calculated from (G.1), if the method of sweeping through the space-time mesh described previously is used. The difficulty may be avoided by evaluating

$$U_2^{n+1/2},\ R_2^{n+1},\ V_{3/2}^{n+1},\ V_{3/2}^{n+1/2},\ T_{3/2}^{n+1/2} \quad \text{and}$$

$$P_{3/2}^{n+1/2},\ ET_{3/2}^{n+1/2},\ EV_{3/2}^{n+1/2},\ AK_{3/2}^{n+1/2},\ AL_{3/2}^{n+1/2}$$

G.5

initially, and then sweeping the mesh as shown in Table V.

The quantities listed in (G.5) may be determined from equations given previously, with the exception of the luminosity AL at the inner boundary. If this boundary is the center of the star, i.e., $R_1^n = 0$ for all time n, then by symmetry

$$AL_1^n = 0 \qquad \text{G.6}$$

for all n also.

Another boundary condition must be imposed on diffusive energy transfer. Christy (1964) has proposed that this be accomplished by requiring that the surface boundary condition for the time-dependent problem be consistent with that for the time-independent diffusion equation. For a static, gray atmosphere, the solution of the equation of transfer for photons is

$$T^4 = \frac{3}{4} T_e^4 [\tau + q(\tau)]$$

where τ is the optical depth and $q(\tau)$ is a slowly-varying function. The diffusion approximation for the same problem gives

$$T^4 = \frac{3}{4} T_e^4 [\tau + c]$$

where c is some constant. If $c = 2/3$ then

$$\left.\frac{\partial (T^4)}{\partial \tau}\right|_{\text{Surface}} = \frac{3}{4} T_e^4 = \frac{3}{2} T^4 \Big|_{\text{Surface}}$$

If the effective temperature T_e of the surface is known, the problem is determined. This may be expressed as

$$\left.\frac{\partial(\log T^4)}{\partial \tau}\right|_{\text{Surface}} = \frac{3}{2}$$

but to apply this expression it is necessary to know where the surface is.

In order to avoid prejudging the calculation, a different approach was taken to determine the surface boundary condition.

When the mean free paths per zone reached a certain small fraction X, a simple energy transfer calculation was made. The incident flux upon zone j+1/2 was obtained from the luminosity at boundary j while the opacity of zone j+1/2 was determined by the temperature of this flux, i.e., the temperature of zone j-1/2. This gave the energy deposited while the neutrino loss rates discussed in chapter III gave the energy emitted by the zone j+1/2. Using (A.13) with the change

$$\dot{s}^{n+1/2}_{j+1/2} \rightarrow \Delta E^{n+1/2}_{j+1/2}$$

where $\Delta E^{n+1/2}_{j+1/2}$ is the net energy deposited by neutrinos, the temperature of zone j+1/2 in the emission surface was determined. In practice the transition from opaque to trans-

parent was so abrupt that the calculation was not sensitive to any sort of reasonable boundary condition of either of the types just mentioned. Outside the emission surface the uncoupled hydrodynamic scheme was used, without any diffusive energy transfer.

H. Stability of the Difference Equations With Radiative Transfer. Richtmyer (1957) has discussed the stability of finite difference approximations to the diffusion equation in some detail. The discussion in this section is therefore limited to those aspects of stability of immediate interest. A complete treatment of the stability of a nonlinear diffusion equation coupled with the equations of hydrodynamics would be extremely complex. It appears that in practice the restrictions necessary for a linear, uncoupled diffusion problem can be suitably generalized for more complex systems.

The simple form of the diffusion equation is

$$\frac{\partial C}{\partial t} = D \frac{\partial^2 C}{\partial x^2}$$

in one dimension, where C is the concentration of whatever is diffusing, t the time, x the spatial coordinate and D the diffusion coefficient. Perhaps one of the simplest difference approximations is

$$\frac{c_j^{n+1} - c_j^n}{\Delta t^{n+1/2}} = D_j^{n+1/2} \quad \frac{c_{j+1}^n - 2c_j^n + c_{j-1}^n}{(\Delta x^2)_j^n}$$

where the subscripts and superscripts have the same meaning as before, and

$$(\Delta x^2)_j^n = (\Delta x_{j+1/2}^n + \Delta x_{j-1/2}^n)^{2/4}$$

For stability it is necessary that*

$$\frac{2D\Delta t}{(\Delta x)^2} \leq 1$$

H.1

for all j and n. This expression may be used to determine the time step $\Delta t^{n+3/2}$ at the next epoch. In particular, for the coupled problem, (H.1) gives

$$\Delta t^{n+3/2} = \frac{ET_{j-1/2}^{n+1/2} \; AK_{j-1/2}^{n+1/2} \; (R_j^{n+1} - R_{j-1}^{n+1})^2}{2(V_{j-1/2}^{n+1/2})^2 \quad (T_{j-1/2}^{n+1/2})^3} \times \text{const.}$$

H.2

which worked quite well when the minimum value for j = 1,. . . JJ was taken.

---

* See Richtmyer 1957, chapters 1 and 6.

T A B L E I

	Condensed model	n = 3 polytrope model
escape velocity for ejected matter	$\sim 1.4 \times 10^{8}$ cm/sec	$\sim 4 \times 10^{8}$ cm/sec
"velocity of ejected matter"	$\sim 7 \times 10^{9}$ cm/sec	$\sim 10^{9}$ cm/sec
mass of remnant core	1.2 $M_{\odot}$	1.8 $M_{\odot}$
radius of core	1.6×10^{6} cm	1.4×10^{6} cm
kinetic energy of ejected mass	$\geq 4 \times 10^{52}$ ergs	$\geq 1.4 \times 10^{52}$ ergs
energy of emitted electron neutrinos	$\sim 7 \times 10^{52}$ ergs	$\sim 6 \times 10^{52}$ ergs

T A B L E II

total light emitted	<< kinetic energy	
intrinsic maximum visual magnitude	-17.5	
mass ejected	≥ 5	$M_\odot$
velocity of ejection	$\sim 7 \times 10^8$	cm/sec
kinetic energy of ejected mass	$\geq 10^{52}$	ergs

T A B L E III

T_9	$\left(-\dot{s}_{\text{decay}}\right)$	$\left(-\dot{s}_{\text{pair-annih.}}\right)$	$\left(-\dot{s}_{\text{tables}}\right)$ *
360	5×10^{24}	3×10^{25}	1.4×10^{26}
240	3.7×10^{22}	4×10^{23}	8×10^{23}
120	1.3×10^{21}	5×10^{18}	2.6×10^{18}

* These values are derived from the Chiu (1961) tables of electron pair-annihilation neutrino rates.

T A B L E IV

T_9	τ
360	10^{-6} sec
240	1.4×10^{-4} sec
120	10^{-2} sec

T A B L E V

quantity	time epoch	space point
U	n+1/2	j+1
R	n+1	j+1
V	n+1	j+1/2
	n+1/2	j+1/2
T	n+1/2	j+1/2
P	n+1/2	j+1/2
ET	n+1/2	j+1/2
EV	n+1/2	j+1/2
AK	n+1/2	j+1/2
AL	n+1/2	j
T	n+1	j-1/2
P	n+1	j-1/2

References

Adams, J. B., M. A. Ruderman, and C. H. Woo. 1963. Phys. Rev. 129, 1383.

Allen, C. W. 1963. Astrophysical Quantities, 2nd ed., The Athlone Press.

Bahcall, J. N. 1964a. Phys. Rev. 136, B1164.

Bahcall, J. N. and S. C. Frautschi. 1964b. Phys. Rev. 136, B1547.

Bahcall, J. N. 1964c. Astrophys. J. 139, 318.

Bahcall, J. N. and R. A. Wolf. 1965. Phys. Rev. Letters 14, 343.

Burgers, J. M. and W. P. Robbertse. 1949. Proc. Koninkl. Ned. Akad. Wetenschap. 52, 1067.

Chandrasekhar, S. 1939. An Introduction to the Study of Stellar Structure, reprinted by Dover Publications, Inc., 1957.

Chiu, H. Y. and R. C. Stabler. 1961. Phys. Rev. 122, 1317.

Chiu, H. Y. 1961. Phys. Rev. 123, 1040.

Chiu, H. Y. 1964. NASA Stellar Evolution Conference held at Institute for Space Studies, in press.

Christy, R. 1964. Rev. Mod. Phys. 36, 555.

Colgate, S. A. and R. H. White. 1964. "The Hydrodynamic Behavior of Supernovae Explosions," UCRL-7777. To be published in the Astrophys. J., 1966.

Davis, R., Jr. 1965. Private communication to A. G. W. Cameron.

Deinzer, W., E. Salpeter. 1964. Astrophys. J. 140, 499.

Dyson, F. "Hydrostatic Instability of a Star," unpublished.

Euwema, R. N. 1964. Phys. Rev. 133, B1046.

Feynman, R. P. and M Gell-Mann. 1958. Phys. Rev. 109, 193.

Frank-Kamenetskii, D. 1962. Physical Processes in Stellar Interiors, Office of Technical Services, U. S. Department of Commerce, Washington 25, D. C., translation from the Russian.

Fowler, W. A. and F. Hoyle. 1964. "Neutrino Processes and Pair Formation in Massive Stars and Supernovae" J. Supplement 91, vol. IX, 201.

Gomes, L. C., J. D. Walecka, and V. F. Weisskopf. 1958. Ann. Phys. 3, 241.

Hansen, C. 1964. unpublished.

Harrison, B., K. Thorne, M. Wakano and J. A. Wheeler. 1965. Gravitational Theory and Gravitational Collapse, University of Chicago Press, Chicago, Ill.

Hayashi, C., R. Hoshi and D. Sugimoto. 1962. Progress of Theoretical Physics, Supplement 22.

Henyey, L. L., L. Wilets, K. H. Bohm, R. LeLevier, and R. D. Levee. 1959. Astrophys. J. 129, 628.

Hofmeister, E., R. Kippenhahn and A. Weigert. 1964. Zeitschrift für Astrophysik 60, 57.

Inman, C. L. and M. A. Ruderman. 1964. Astrophys. J. 140, 1025.

Landau, L. D. and E. M. Lifshitz. 1958. Statistical Physics, Addison-Wesley Publishing Co., Reading, Mass.

Minkowski, R. 1964. Annual Review of Astronomy and Astrophysics, 2, 247.

Richtmyer, R. D. 1957. Difference Methods for Initial Value Problems, Interscience Publishers, Inc., New York.

Ritus, V. I. 1962. Soviet Physics - JETP 14, 915.

Schwarzschild, M. 1958. Structure and Evolution of the Stars, Princeton University Press, Princeton, N. J.

Sedov, L. I. 1959. Similarity and Dimensional Methods in Mechanics, Academic Press, New York.

Shklovskii, I. S. 1960. Soviet Astronomy - AJ V, 355.

Stothers, R. 1966. Astrophys. J. 143, 91.

Truran, J. W., C. J. Hansen, A. G. W. Cameron and A. Gilbert. 1966. Can. J. Phys. 44, 151.

Tsuruta, S. 1964. Ph. D. Thesis, Columbia University.

Von Neumann, J. and R. D. Richtmyer. 1950. Journal of Applied Physics 21, 232.

Figure Captions

Figure 1. Zero temperature equation at State.

Figure 2. Comparison of the structure of isothermal-core and polytrope of index 3 models in the temperature - density plane.

Figure 3. Comparison of the structure of isothermal-core and polytrope of index 3 models in the radius - density plane.

Figure 4. Evolutionary historyof M_r = 1.5 $M_\odot$ zone of 10 $M_\odot$ polytrope of index 3, for three different treatments of neutrino energy transfer.

Figure 5. Evolutionary history of two representative mass zones of a 10 $M_\odot$ polytrope of index 3 initial model, with neutrino energy transfer treated in the diffusion approximation.

Figure 6. Comparison with the calculations of Colgate and White.

Figure 7. Temperature-density history of two representative zones of the isothermal-core initial model, with energy transfer by neutrinos in the diffusion approximation.

Table Captions

Table I. Comparison of centrally-condensed and polytropic models.

Table II. Observed characteristics of type II supernovae.

Table III. Estimates of energy loss in ergs/gm/sec due to muon-type neutrinos formed by muon-decay and muon pair-annihilation (density is $\rho = 10^{12}$ gm/cm^3).

Table IV. Relaxation time for cooling due to muon-type neutrino escape at high temperature (density is $\rho = 10^{12}$ gm/cm^3).

Table V. Space-time points at which quartities appearing in the coupled difference equations of hydrodynamics and diffusive energy transfer are evaluated.